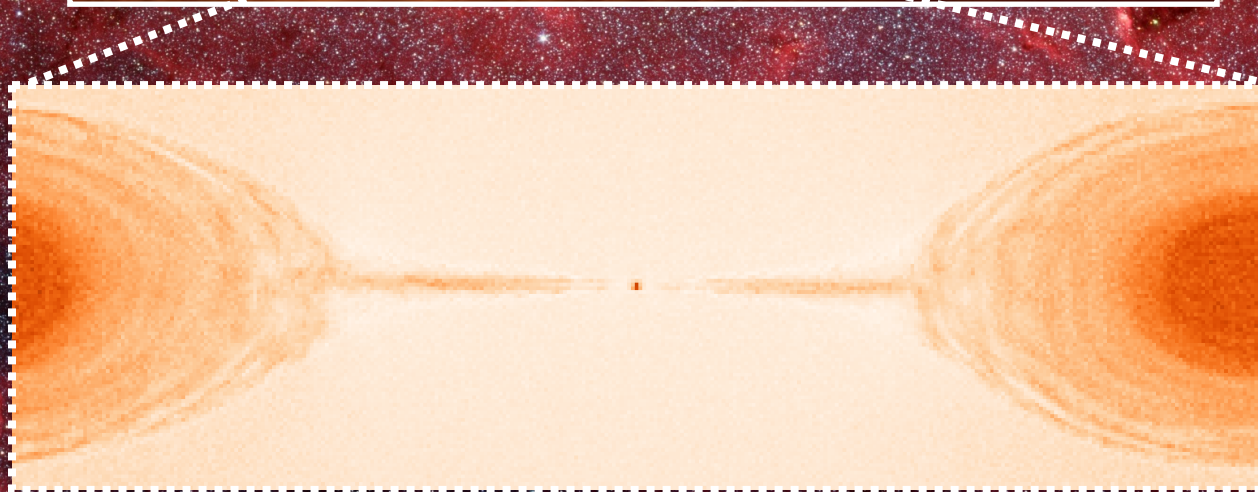
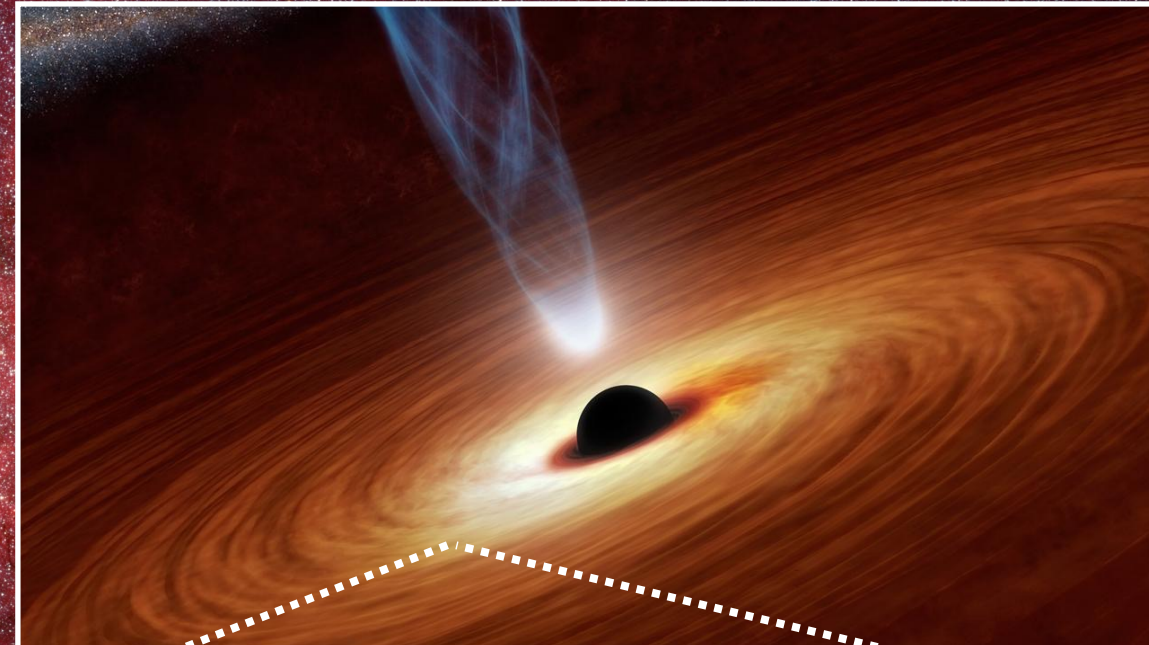


# Electron Heating in Quasi-Relativistic Magnetic Reconnection

Michael Rowan

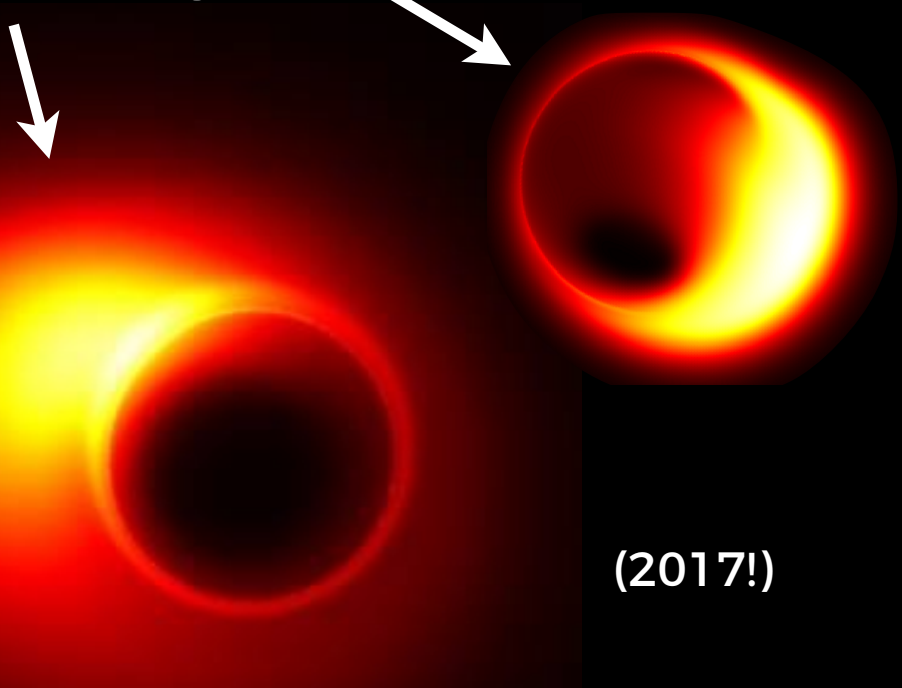
Collaborators: Ramesh Narayan, Lorenzo Sironi

12/16/2016

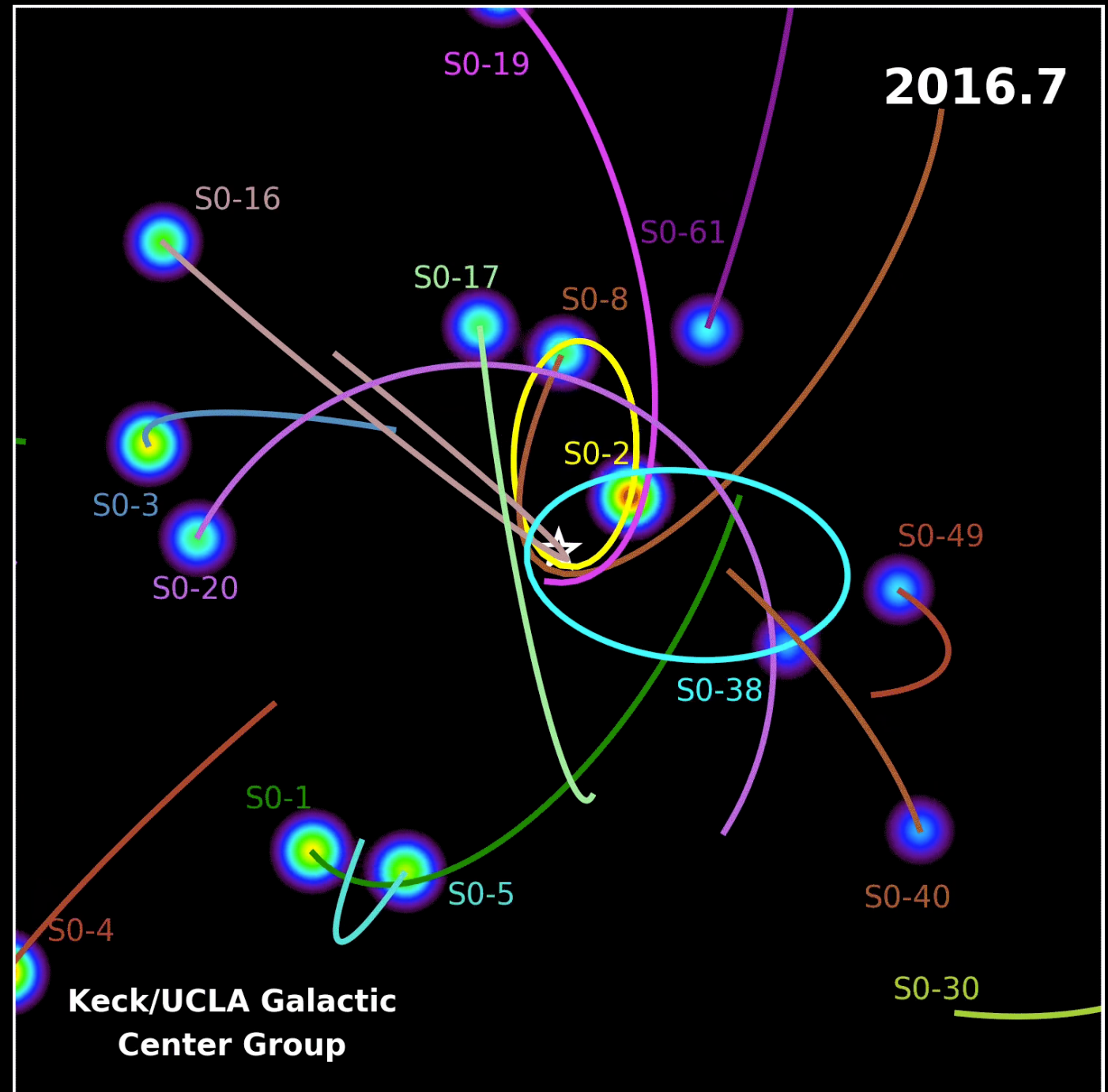


# The importance of black holes

- ▶ Highly energetic
  - ▶ Quasars
  - ▶ GRBs
- ▶ Feedback into environment
  - ▶ Galaxy evolution
  - ▶ Large-scale structure
- ▶ EHT
  - ▶ Image black holes
  - ▶ M87, Sgr A\*



(2017!)

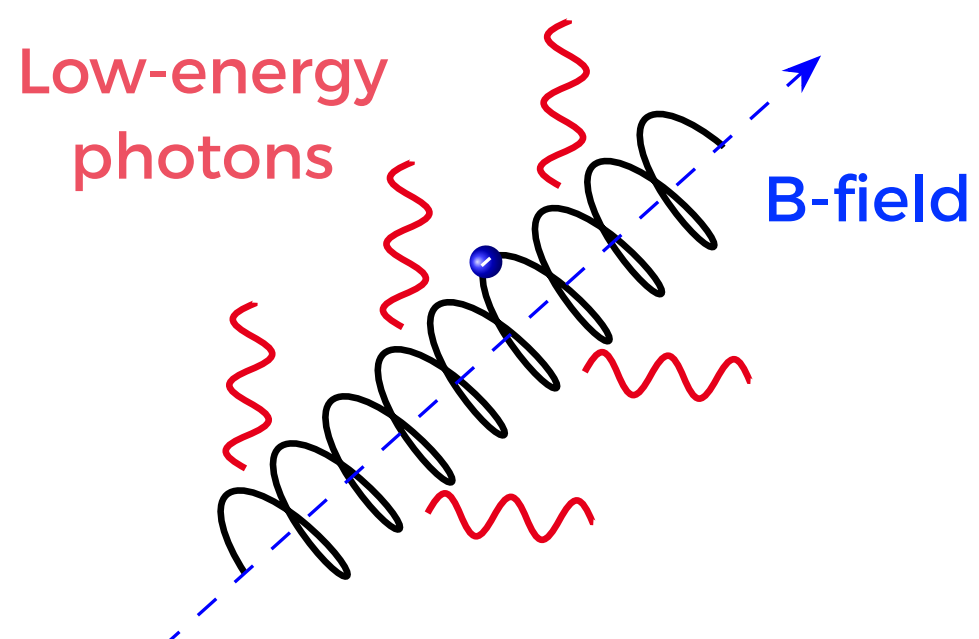


Credit: A. E. Broderick

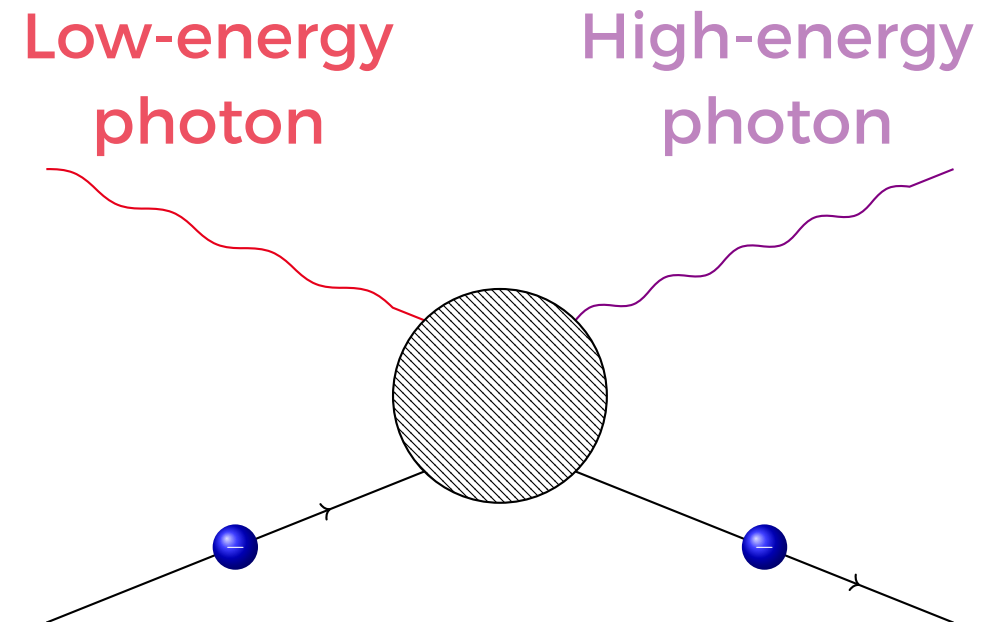
# Electrons in accretion disk make radiation

Energetic electrons can produce radiation through various processes:

## Synchrotron



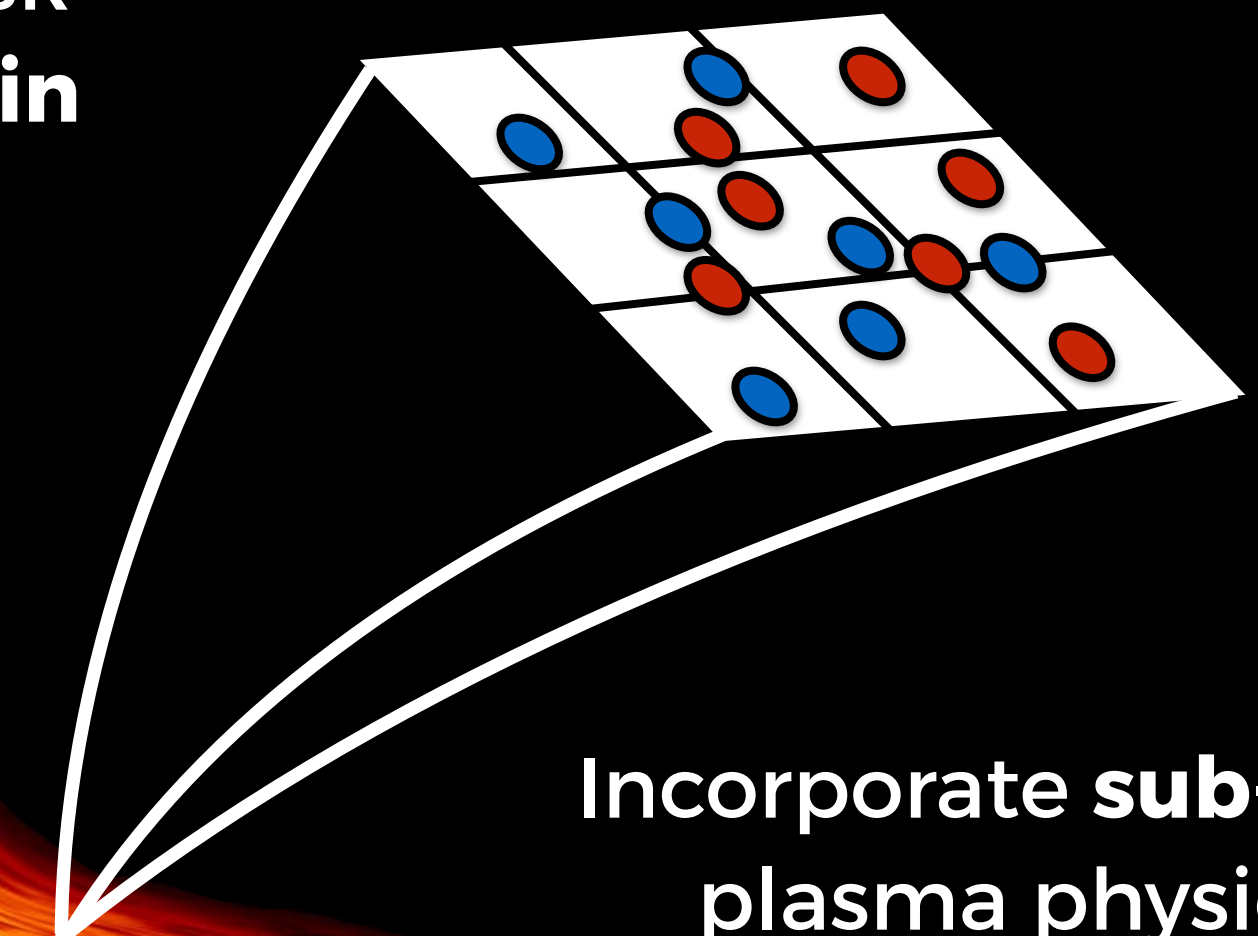
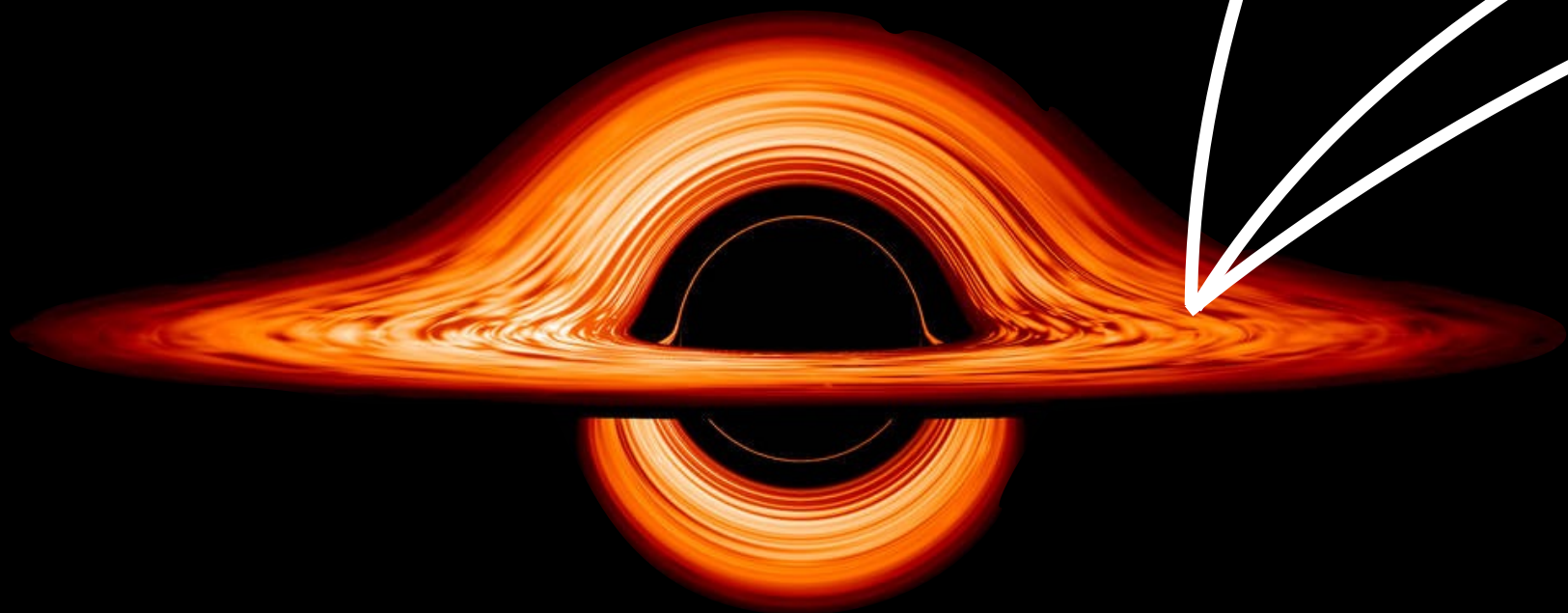
## Inverse Compton



Electrons are responsible for observed radiation profiles, yet the production of energetic electrons is **unresolved** in global simulations

# How can we make global simulations more complete?

Global fluid simulations of collisionless accretion disk radiation are **potentially in great error**



Incorporate **sub-grid plasma physics**

- ▶ Reconnection
- ▶ Shocks

# Reconnection can energize particles

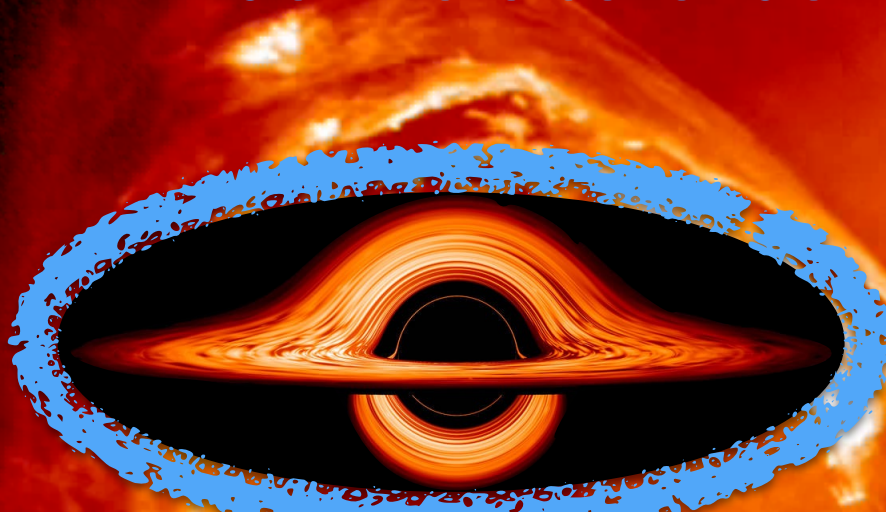
- ▶ Rearrangement of magnetic field lines
- ▶ Magnetic energy → particle kinetic energy

# Reconnection can energize particles

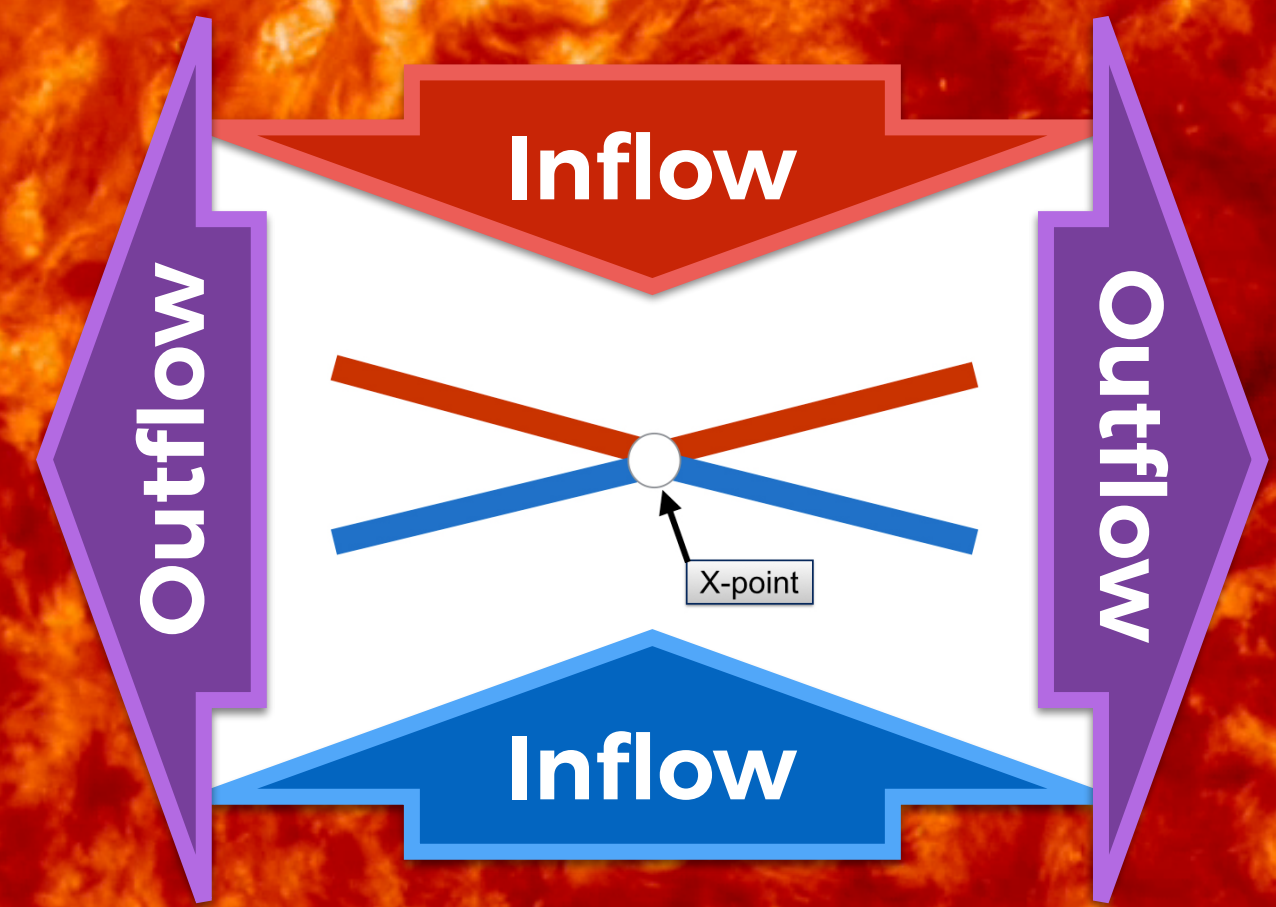
- ▶ Rearrangement of magnetic field lines
- ▶ Magnetic energy → particle kinetic energy

Happens many places:

Chromosphere  
Magnetosphere  
**Black hole coronae**



NASA GSFC/J. Schnittman



NASA SDO

# Parameters: physical and computational

## beta (of the ions)

$$\beta_i = \frac{n_i k_B T_i}{B^2 / (8\pi)} = \frac{\text{thermal pressure}}{\text{magnetic pressure}}$$

## sigma (of the ions)

$$\sigma_i = \frac{B^2 / (4\pi)}{n_i m_i c^2} = \frac{\text{magnetic pressure } (\times 2)}{\text{rest-mass energy density}}$$

## temperature ratio

$$\frac{T_e}{T_i} = \frac{\text{electron temperature}}{\text{ion temperature}}$$

## Computational

$d_{\text{stripe}}$

$dv_{\text{stripe}}$

$n_{\text{stripe}}$

$m_y$

$n_{\text{times}}$

$m_i/m_e$

$ppc$

$c/\omega_{pe}$

# Full relativistic definition of sigma includes enthalpy

## sigma, including enthalpy

$$\sigma_w = \frac{\frac{m_i}{m_e} + 1}{\frac{m_i}{m_e} \left( 1 + \frac{\hat{\gamma}_i - 1}{\hat{\gamma}_i - 1} \frac{k_B T_i}{m_i c^2} \right) + \left( 1 + \frac{\hat{\gamma}_e - 1}{\hat{\gamma}_e - 1} \frac{k_B T_e}{m_e c^2} \right)} \frac{B^2}{4\pi(n_i m_i + n_e m_e)c^2}$$

$\approx 1$  for a cold plasma

$$\approx \frac{B^2}{4\pi n_i m_i c^2} \equiv \sigma_i$$

For a high-beta (thermally ‘hot’) plasma, the contribution from the thermal pressure is non-negligible

One more important definition:  
Alfvén velocity, which describes  
the speed of magnetic waves

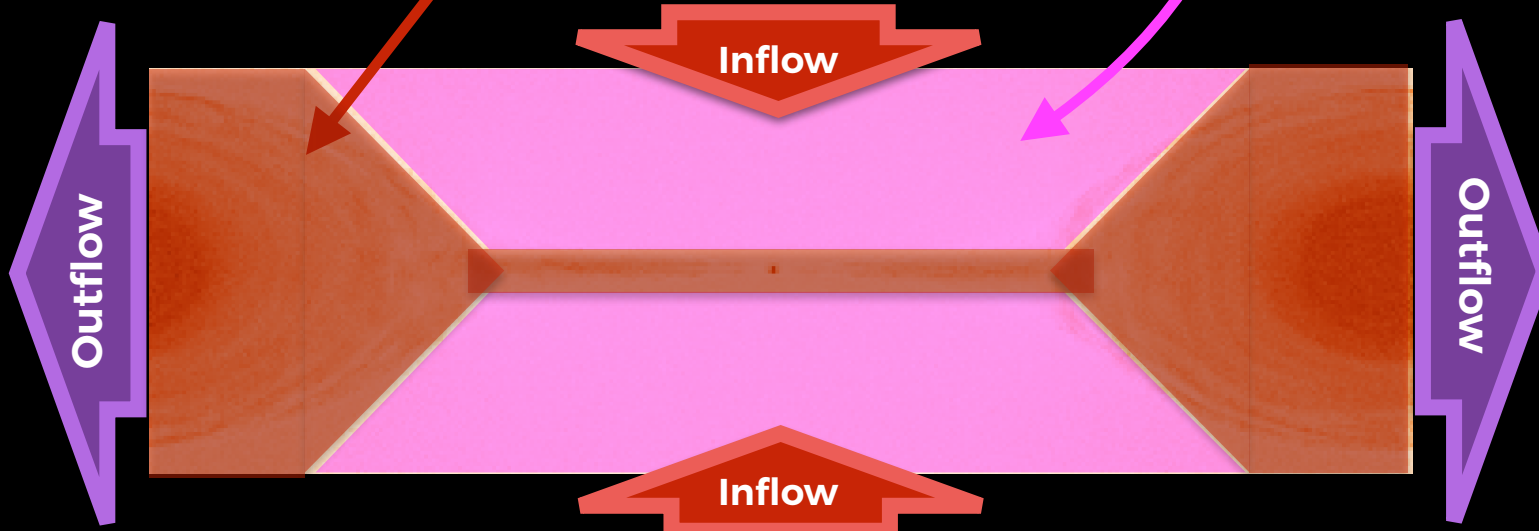
## Alfvén velocity

$$\frac{v_A}{c} = \sqrt{\frac{\sigma_w}{1 + \sigma_w}}$$

# Characterization of heating

A useful number we can extract from each simulation is the following dimensionless ratio:

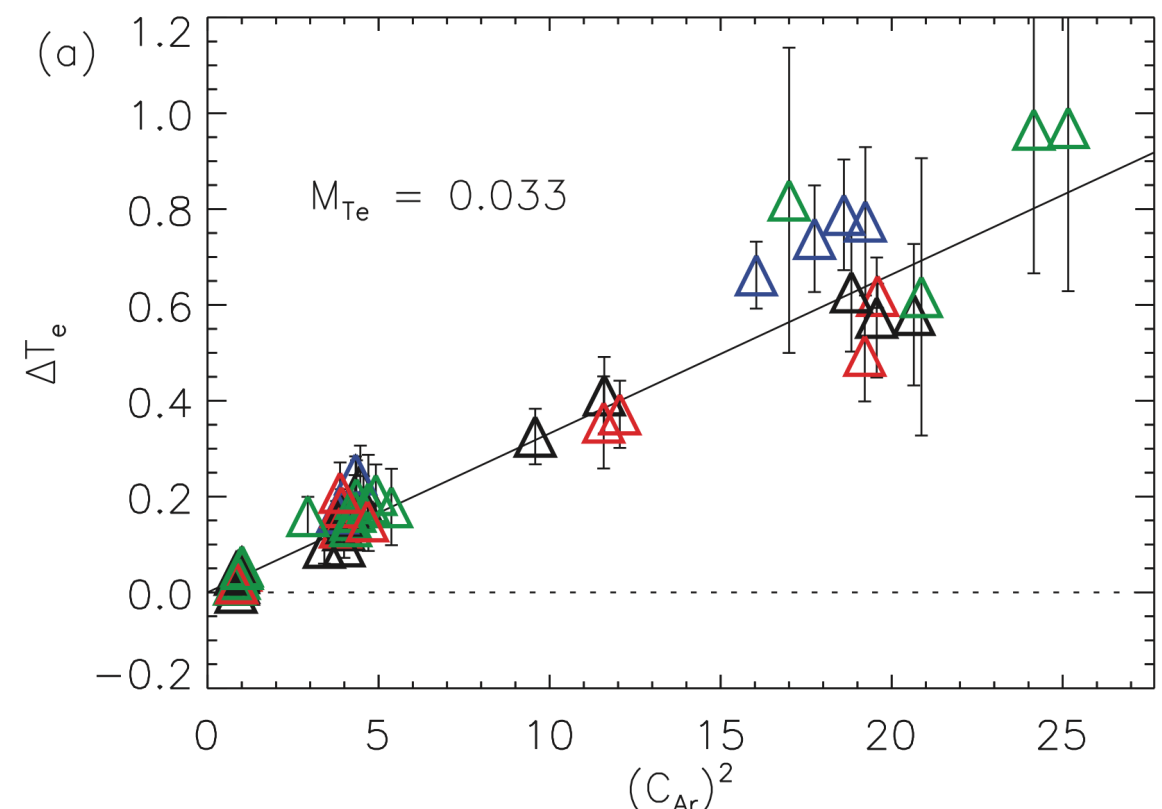
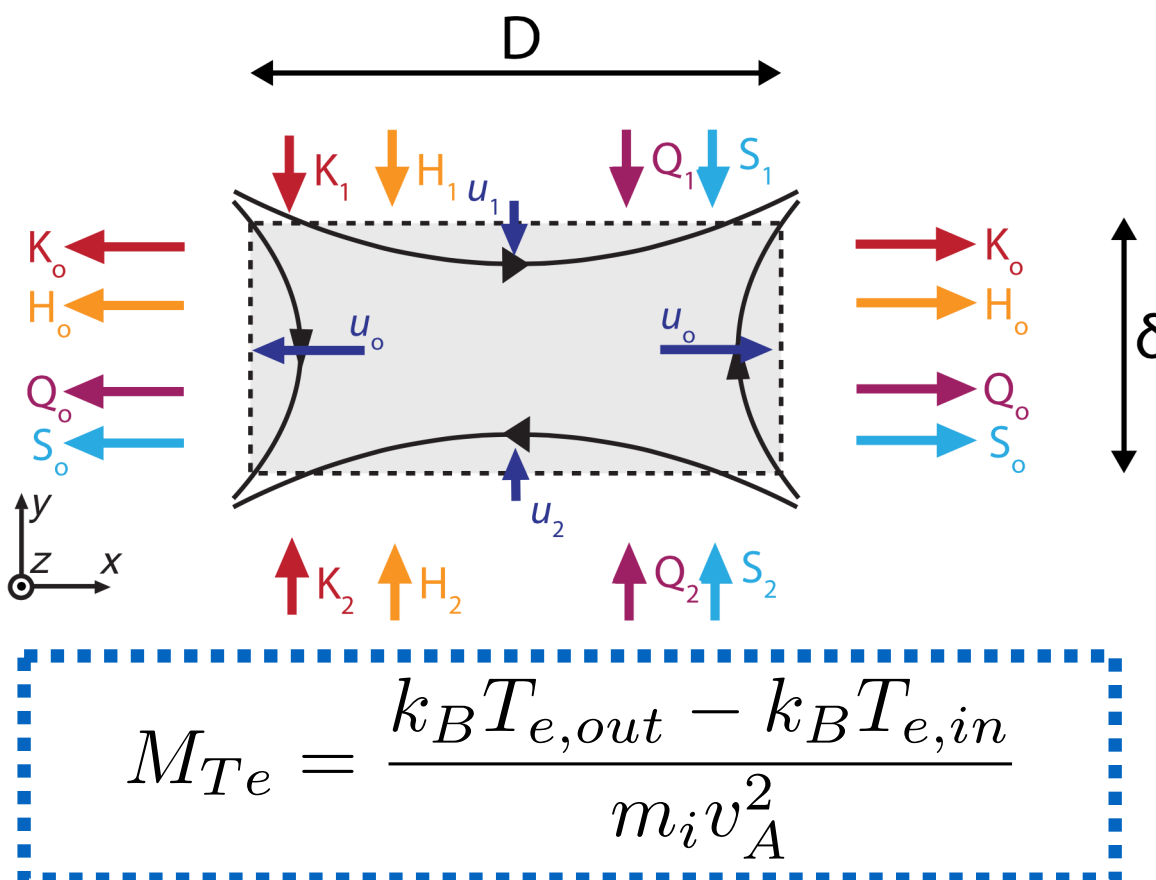
$$M_{Te} = \frac{k_B T_{e,out} - k_B T_{e,in}}{B^2 / (4\pi n)}$$



This is the ratio of increase in temperature to magnetic energy available for dissipation. It can be thought of as the 'efficiency' of reconnection.

# How much are electrons heated during reconnection?

PIC simulations and observations of magnetic reconnection suggest that a constant fraction of inflowing magnetic energy is given to electrons

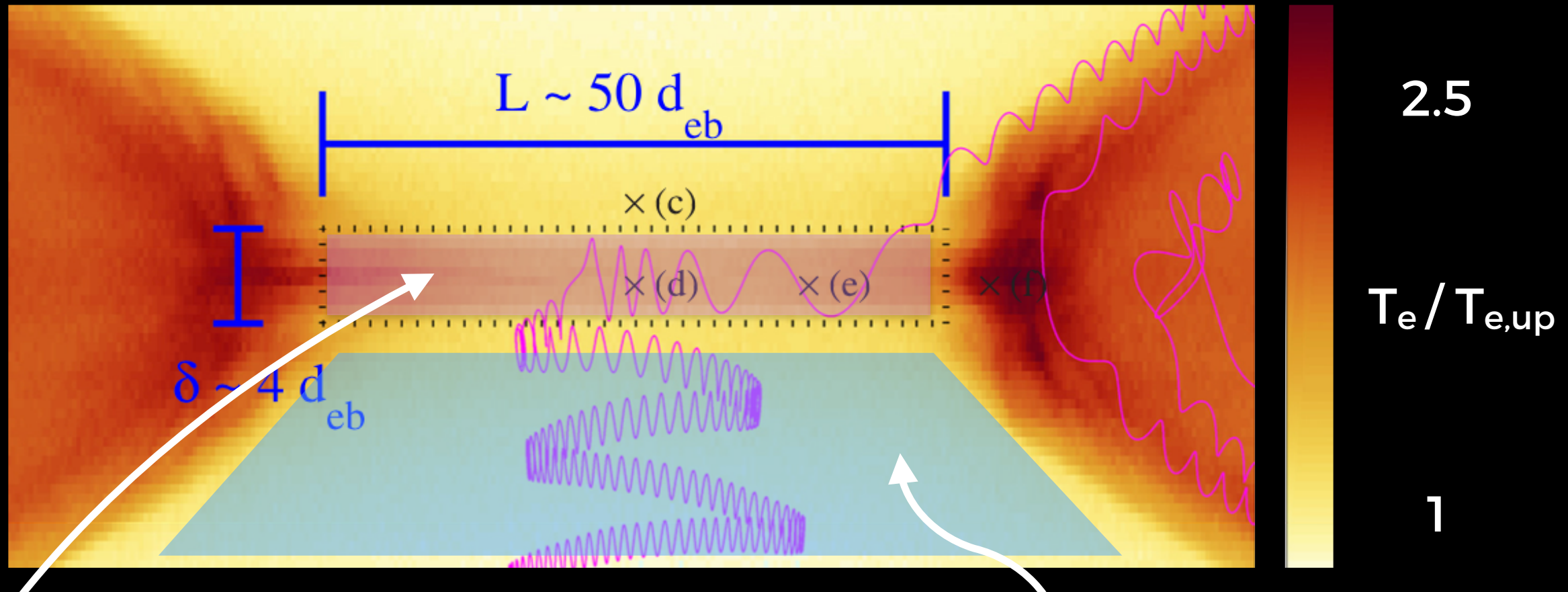


(Drake et al., 2014)

This fraction  $M_{Te}$  is remarkably independent of plasma parameters in the inflowing region

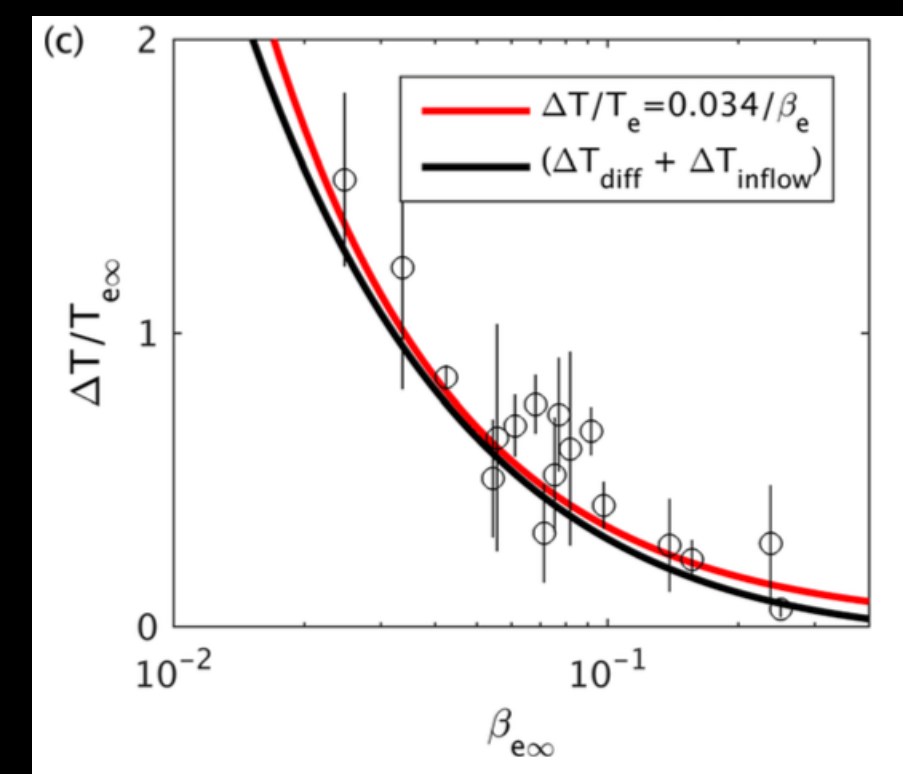
# A model for the heating mechanism exists

(Le et al., 2016)



$$\frac{\Delta T_{e,tot}}{T_{e,up}} = \frac{\Delta T_{e,in}}{T_{e,up}} + \frac{\Delta T_{e,diff}}{T_{e,up}} \simeq \frac{0.034}{\beta_{e,up}}$$

The model (middle terms) agrees  
with the empirical scaling (last term)



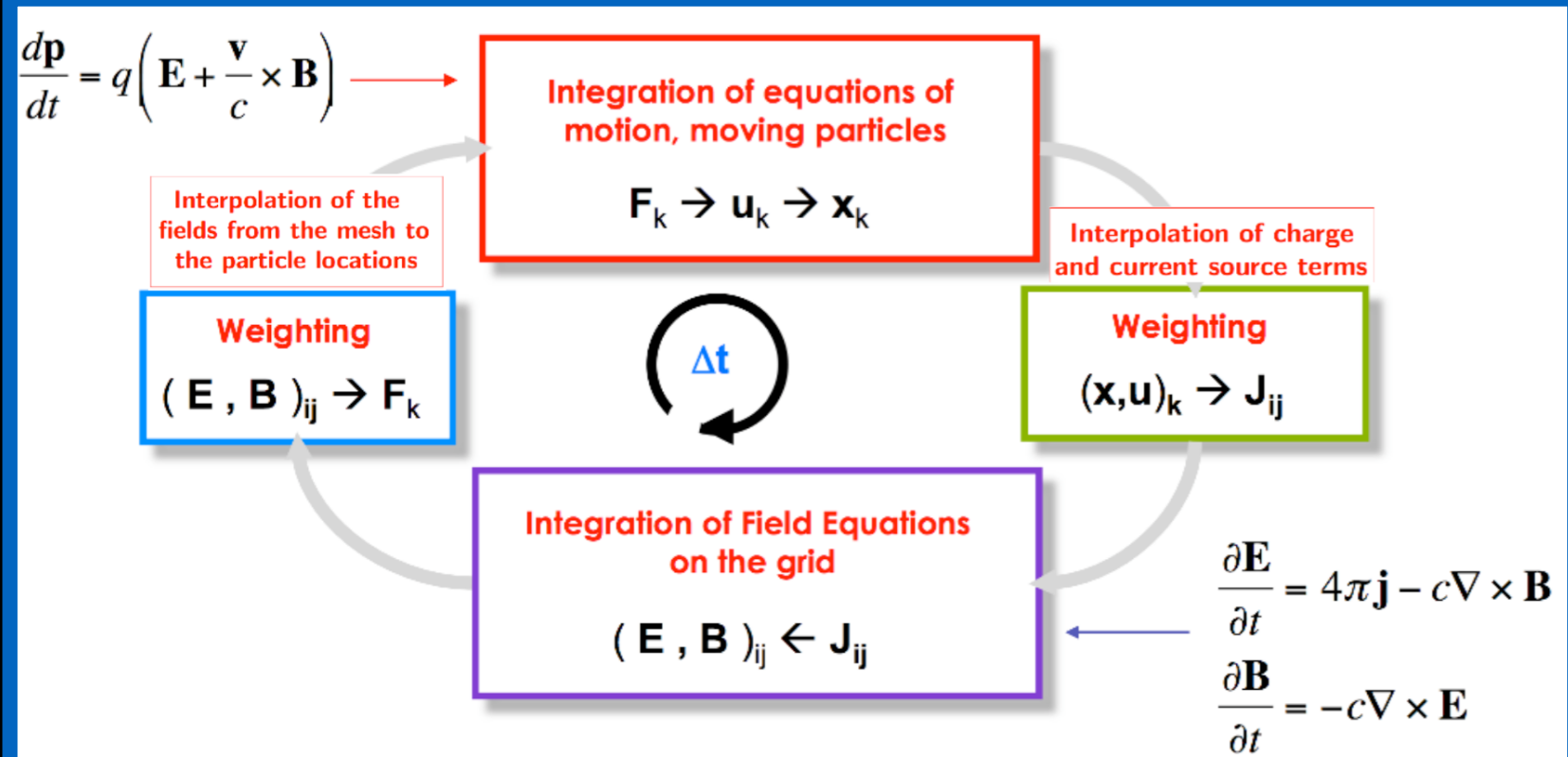
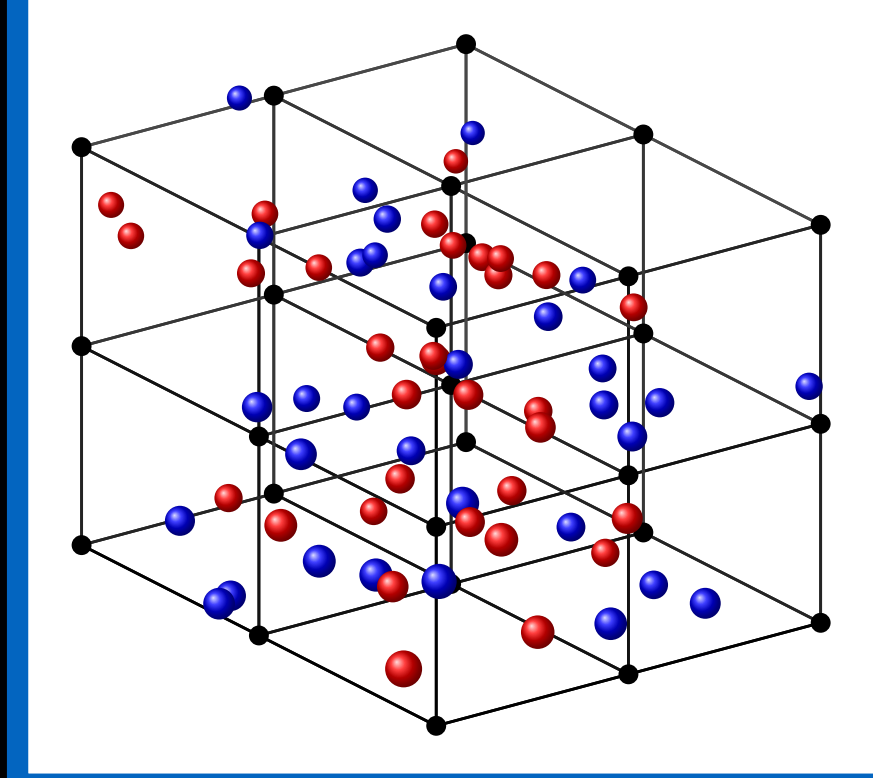
(Le et al., 2016)

# The quasi-relativistic regime is relatively unexplored

## Parameters

$\sigma_w$	$\beta_i$	$T_e/T_i$	$\Delta\gamma_i$
0.1	0.0078125	0.1	0.000406687
0.1	0.0078125	0.3	0.000406767
0.1	0.0078125	1	0.000407051
0.1	0.03125	0.1	0.00163203
0.1	0.03125	0.3	0.00163334
0.1	0.03125	1	0.00163818
0.1	0.125	0.1	0.00661497
0.1	0.125	0.3	0.00663803
0.1	0.125	1	0.00673223
0.1	0.5	0.1	0.0280133
0.1	0.5	0.3	0.0285164
0.1	0.5	1	0.0308345
0.1	2.	0.1	0.155222
0.1	2.	0.3	0.178254
0.1	2.	1	0.394336
0.3	0.0078125	0.1	0.0012227
0.3	0.0078125	0.3	0.00122343
0.3	0.0078125	1	0.0012261
0.3	0.03125	0.1	0.00493921
0.3	0.03125	0.3	0.00495179
0.3	0.03125	1	0.00500182
0.3	0.125	0.1	0.0205981
0.3	0.125	0.3	0.0208554
0.3	0.125	1	0.022019
0.3	0.5	0.1	0.102084
0.3	0.5	0.3	0.110952
0.3	0.5	1	0.163062

Use **PiC simulation**.  
 Choose parameters  
 so that inflow/  
 outflow electrons  
 are **moderately**  
 relativistic



# The Vlasov equation

if they are at about the same position and share about the same velocity. Hence, we define  $f(\mathbf{x}, \mathbf{v}, t)$  as the particle distribution function, which represents the number density of particles found near the point  $(\mathbf{x}, \mathbf{v})$  in phase space. Specifically, the number of particles located within intervals  $d^3x$  about  $\mathbf{x}$  and  $d^3v$  about  $\mathbf{v}$  is given by

$$dN = f(\mathbf{x}, \mathbf{v}, t) d^3x d^3v . \quad (2)$$

$\mathbf{X} \equiv (\mathbf{x}, \mathbf{v})$  is phase space coordinates and  $\dot{\mathbf{X}} = (\mathbf{v}, \mathbf{a})$

$$\dot{\mathbf{x}}_i = \mathbf{v}_i , \quad \dot{\mathbf{v}}_i = \mathbf{a}_i = \frac{q}{m} \left( \mathbf{E} + \frac{\mathbf{v}_i \times \mathbf{B}}{c} \right)$$

$$\frac{\partial f}{\partial t} + \nabla \cdot (f \mathbf{v}) + \nabla_{\mathbf{v}} \cdot (f \mathbf{a}) = 0$$

$$\frac{Df}{Dt} \equiv \left( \frac{\partial}{\partial t} + \dot{\mathbf{X}} \frac{\partial}{\partial \mathbf{X}} \right) f = 0 ,$$

$Df/Dt = 0$  is known as *Liouville's theorem*. It states that the distribution function  $f$  is constant along particle trajectories in phase space (when  $\nabla_{\mathbf{v}} \cdot \mathbf{a} = 0$ ).

# The Vlasov-Maxwell equations

$$\frac{\partial f}{\partial t} + \mathbf{v} \cdot \nabla f + \frac{q}{m} \left( \mathbf{E} + \frac{\mathbf{v}}{c} \times \mathbf{B} \right) \cdot \nabla_{\mathbf{v}} f = \left( \frac{\partial f}{\partial t} \right)_{\text{coll}}$$

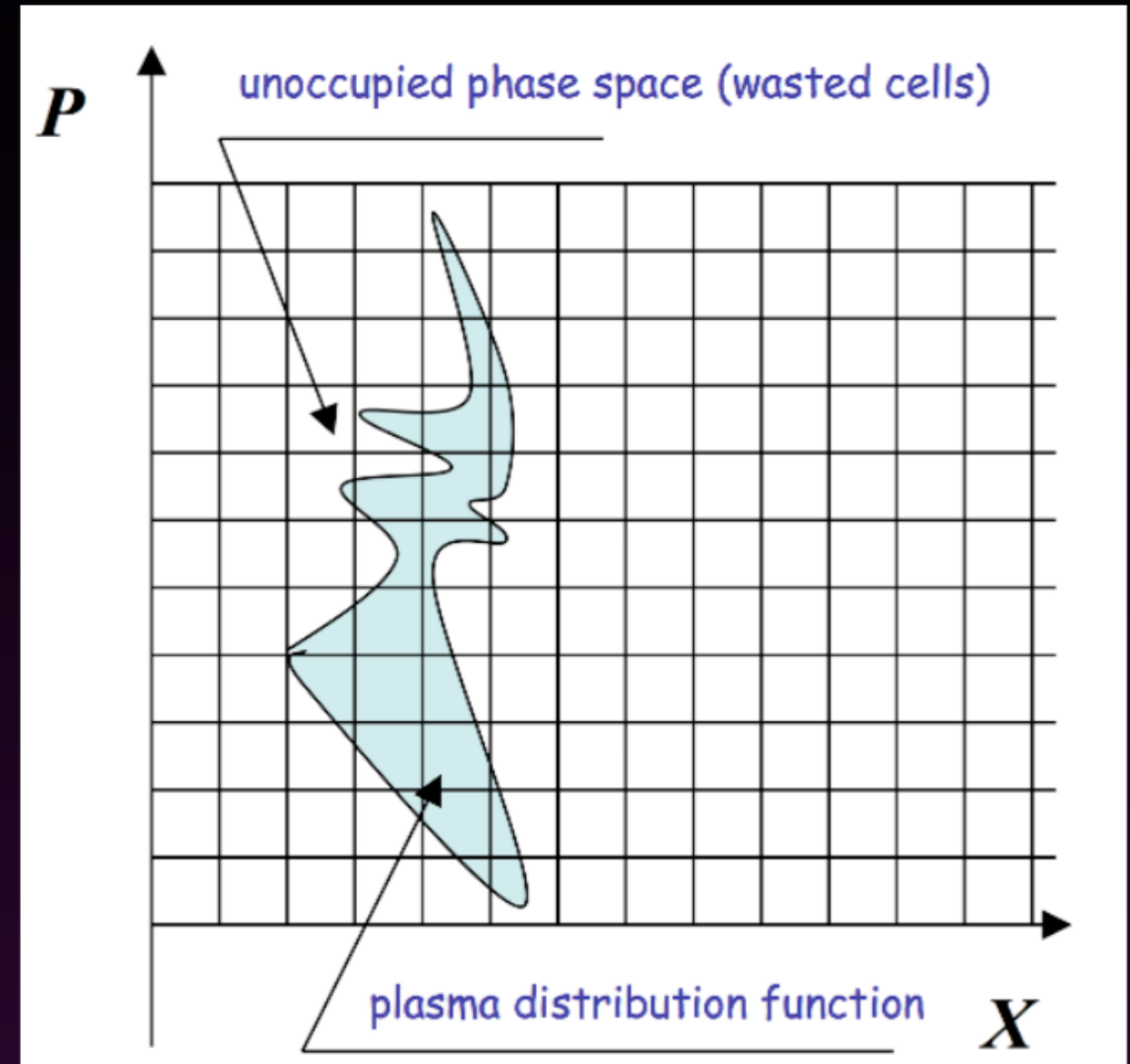
$$\begin{aligned}\frac{1}{c} \frac{\partial \mathbf{E}}{\partial t} &= \nabla \times \mathbf{B} - \frac{4\pi}{c} \mathbf{j} , \\ \frac{1}{c} \frac{\partial \mathbf{B}}{\partial t} &= -\nabla \times \mathbf{E} , \\ \nabla \cdot \mathbf{E} &= 4\pi\rho , \\ \nabla \cdot \mathbf{B} &= 0 .\end{aligned}$$

$$\begin{aligned}\rho &= \sum_{\text{species}} q \int f(\mathbf{x}, \mathbf{v}, t) d^3 v , \\ \mathbf{j} &= \sum_{\text{species}} q \int \mathbf{v} f(\mathbf{x}, \mathbf{v}, t) d^3 v .\end{aligned}$$

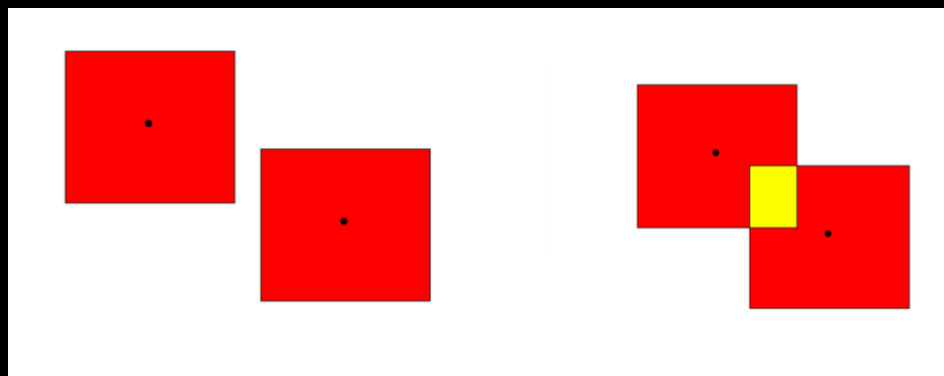
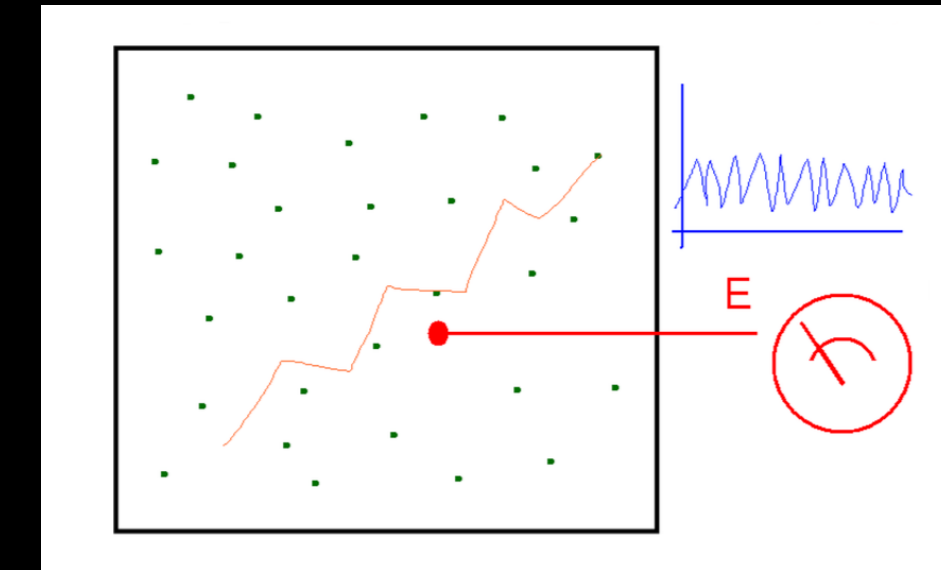
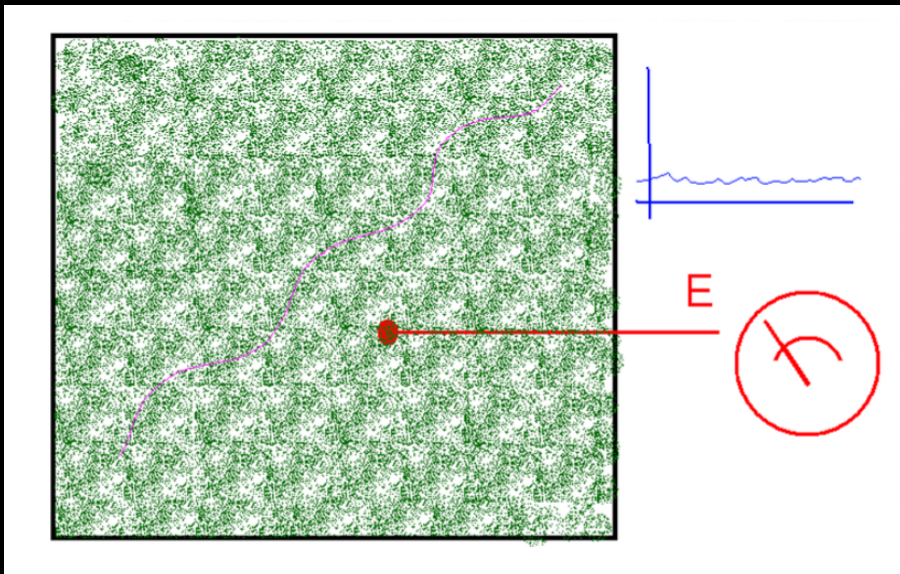
# Solving the Vlasov-Maxwell equations

Two options:

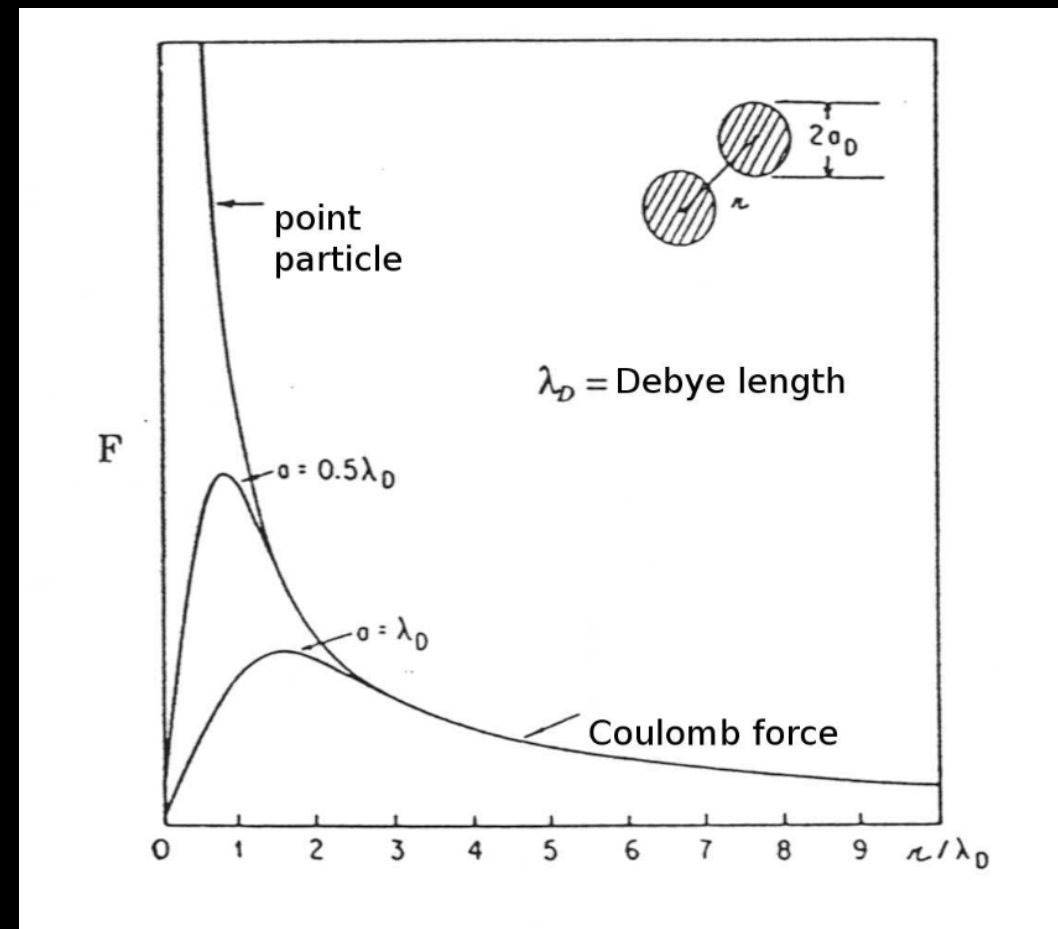
- Discretize the Vlasov equation on a grid in phase space:
  1. computationally expensive to solve in 6+1 dimensions
  2. how to determine the boundaries of the grid in momentum space?
  3. what if  $f < 0$ ?
- Sample the phase space density with particles, and follow them as LAGRANGIAN tracers.



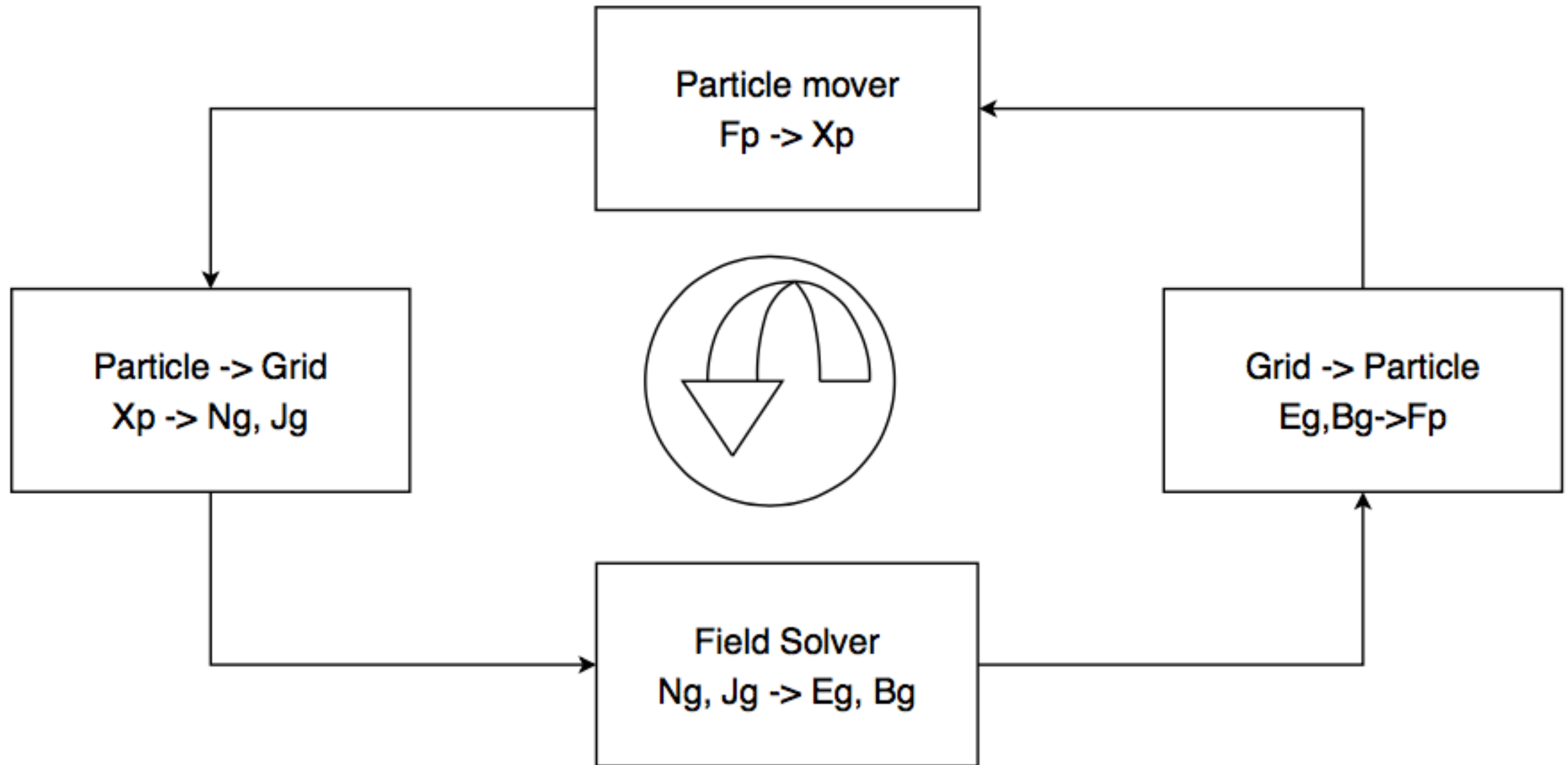
# Macro-particles vs. real particles



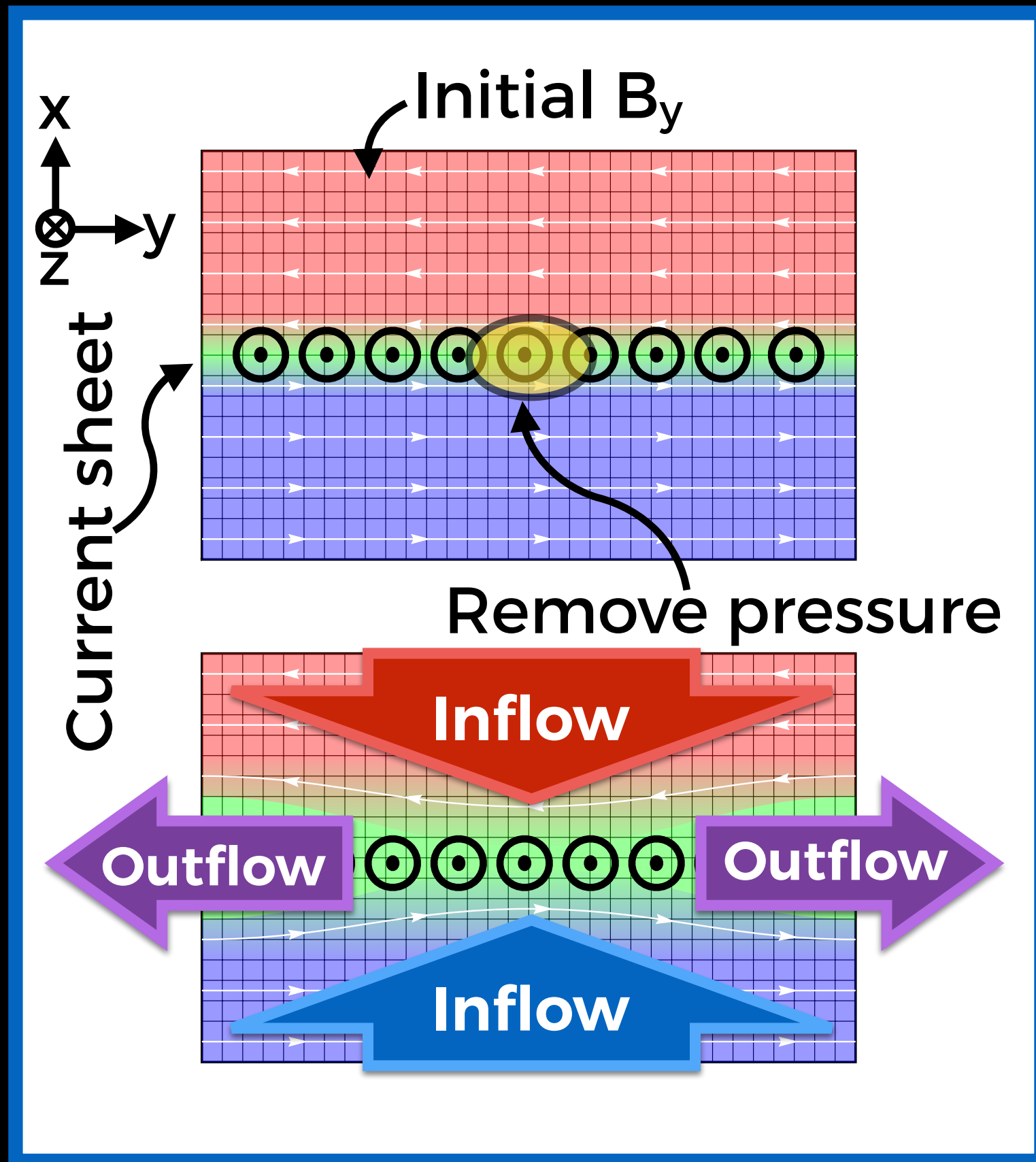
$$\Lambda = \frac{E_{th}}{E_{pot}} = \frac{4\pi\epsilon_0 a k T}{q^2}$$



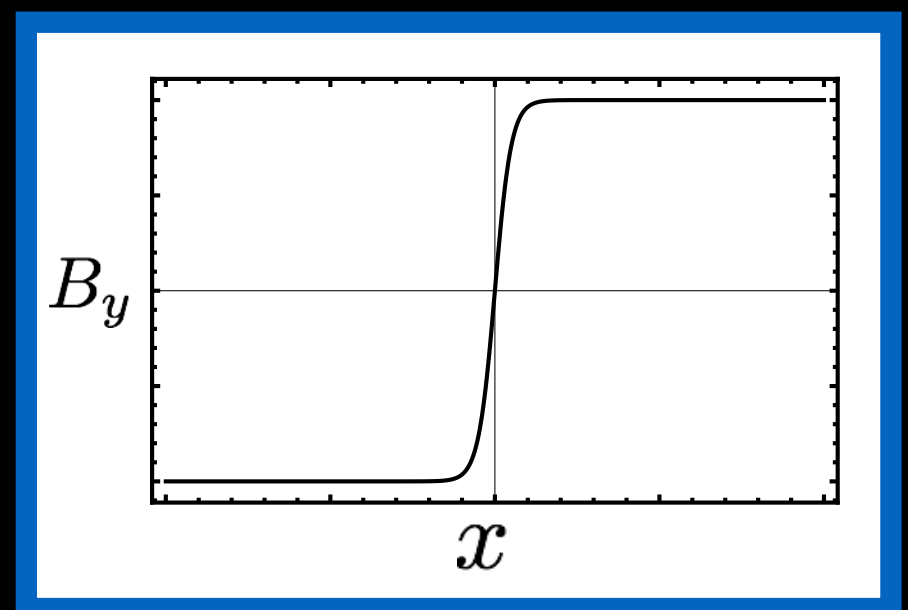
# Particle-in-cell loop



# Start with alternating $\vec{B}$ -field and trigger reconnection



- ▶ B-field initialized in Harris equilibrium



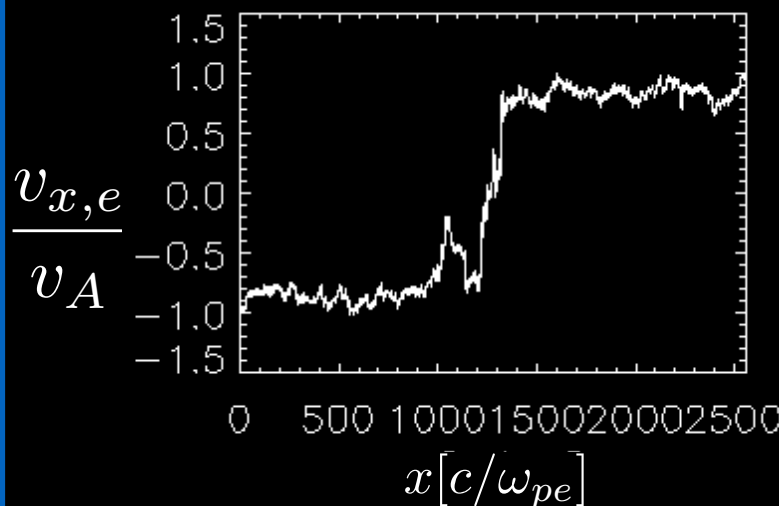
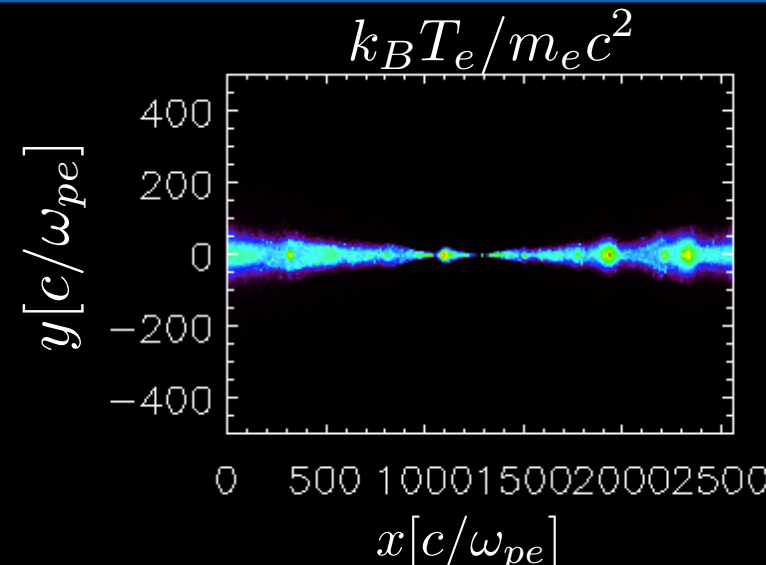
$$\mathbf{B} = B_0 \tanh(x/L) \mathbf{e}_y$$

- ▶ Hot, overdense strip of particles at beginning (green)
- ▶ Remove the particle pressure in center to drive reconnection

# Boundary conditions

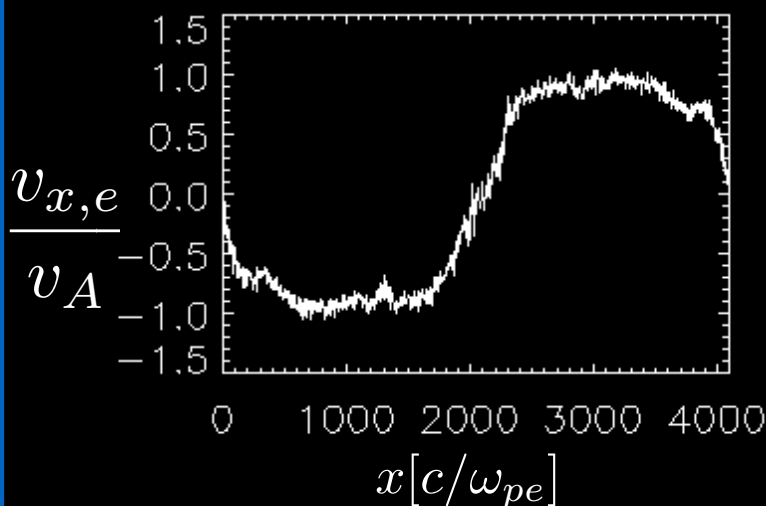
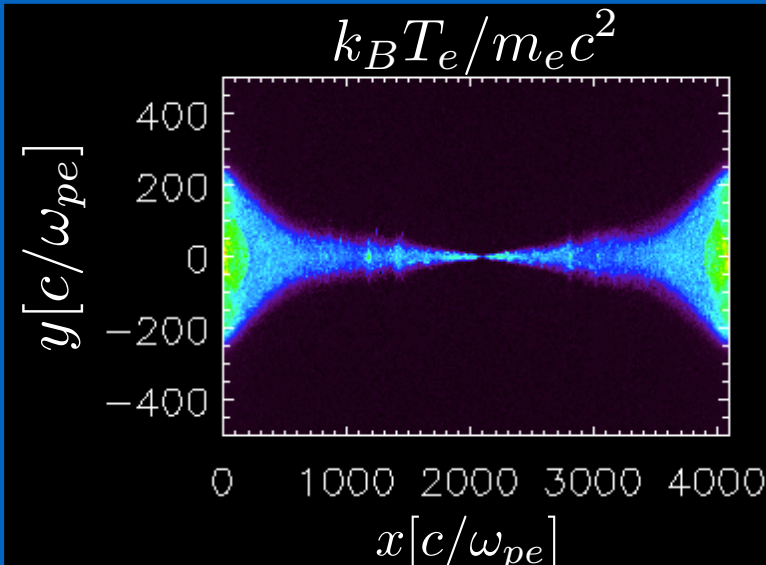
## Outflow

- ▶ Particles escape along x-dir.
- ▶ Allows for study of long-term evolution of system



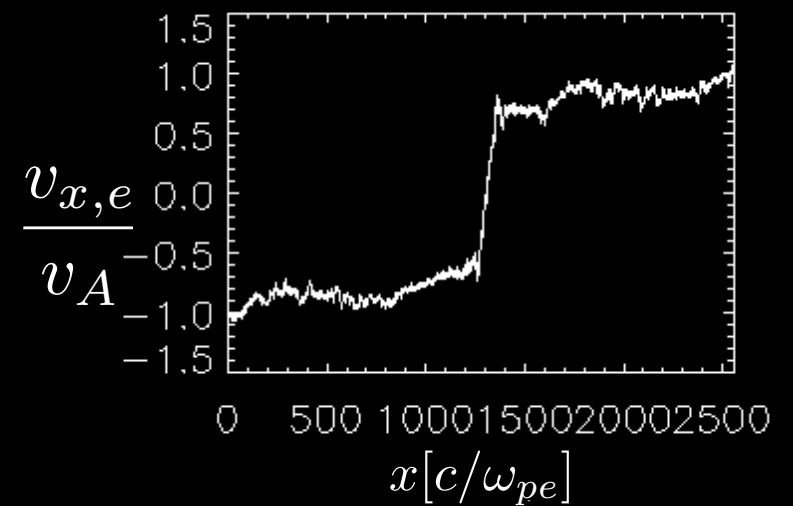
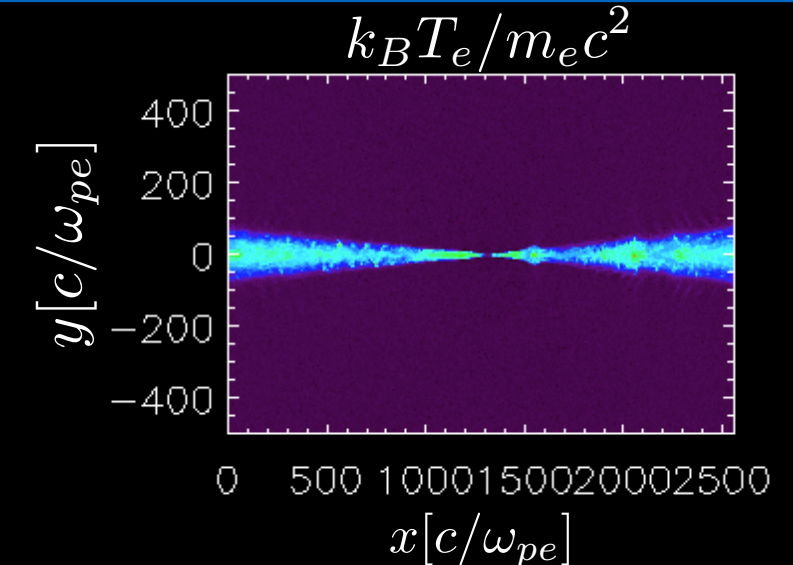
## Periodic

- ▶ No particles are lost
- ▶ However, sensitive to boundaries after  $1/2$  Alfvén crossing-time



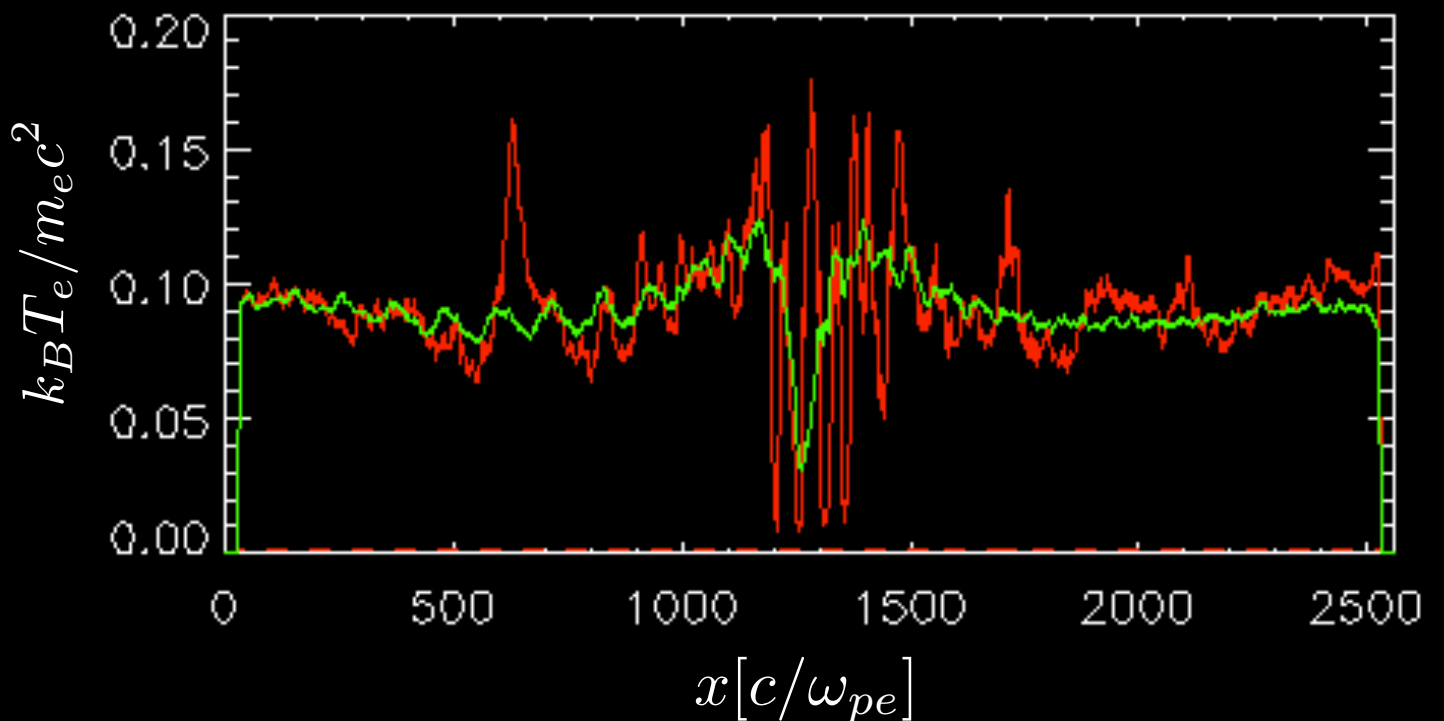
## Adaptive

- ▶ Modified version of outflow boundary condition
- ▶ Includes additional controls necessary for high-beta case



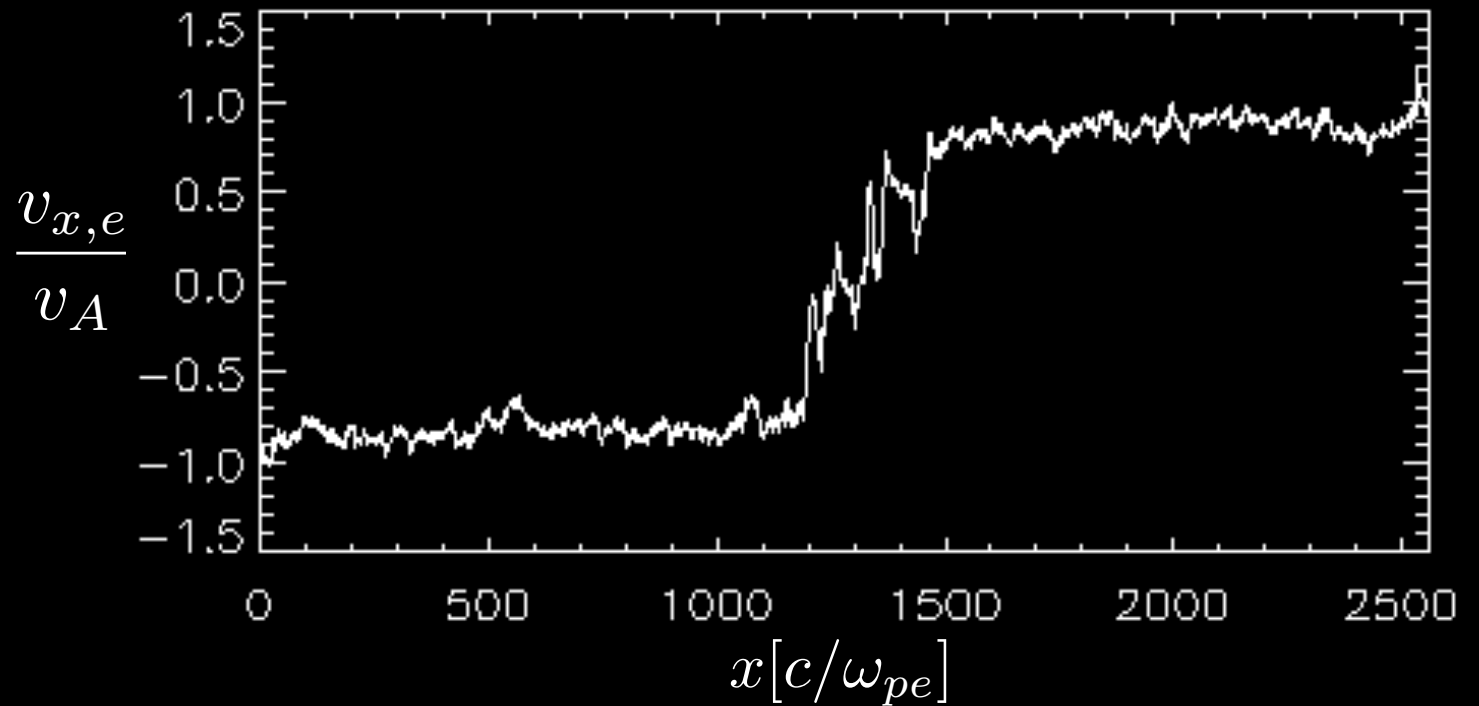
# The plasma reaches a quasi-steady state

- ▶ To extract a meaningful outflow temperature, temperature profile should be flat
- ▶ Alfvén velocity should be saturated in current sheet



## Alfvén velocity

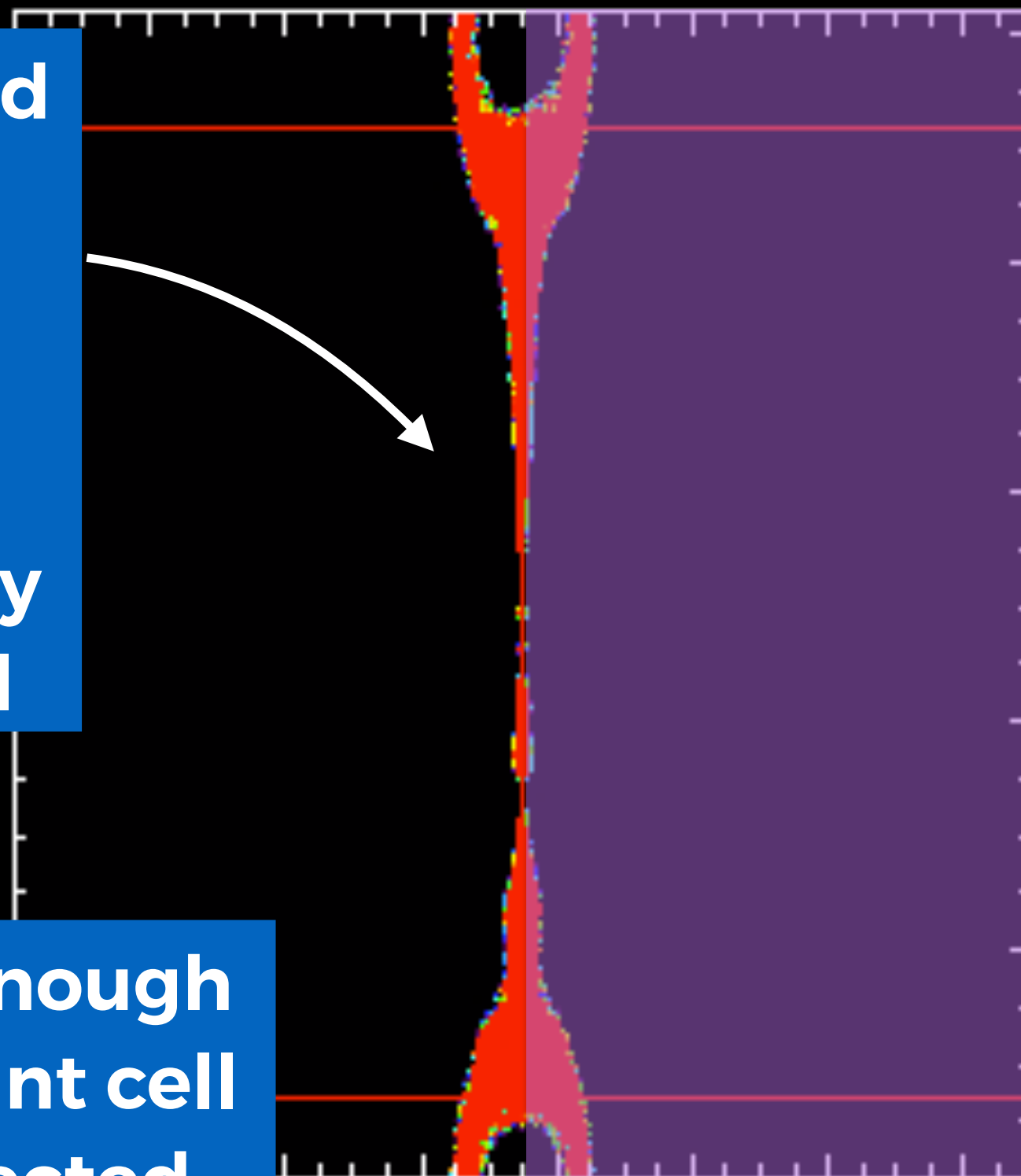
$$\frac{v_A}{c} = \sqrt{\frac{\sigma_w}{1 + \sigma_w}}$$



# How to identify where reconnection has happened?

Track tagged particles;  
measure ratio of  
tagged to total density  
in each cell

If there is enough  
mixing, count cell  
as reconnected

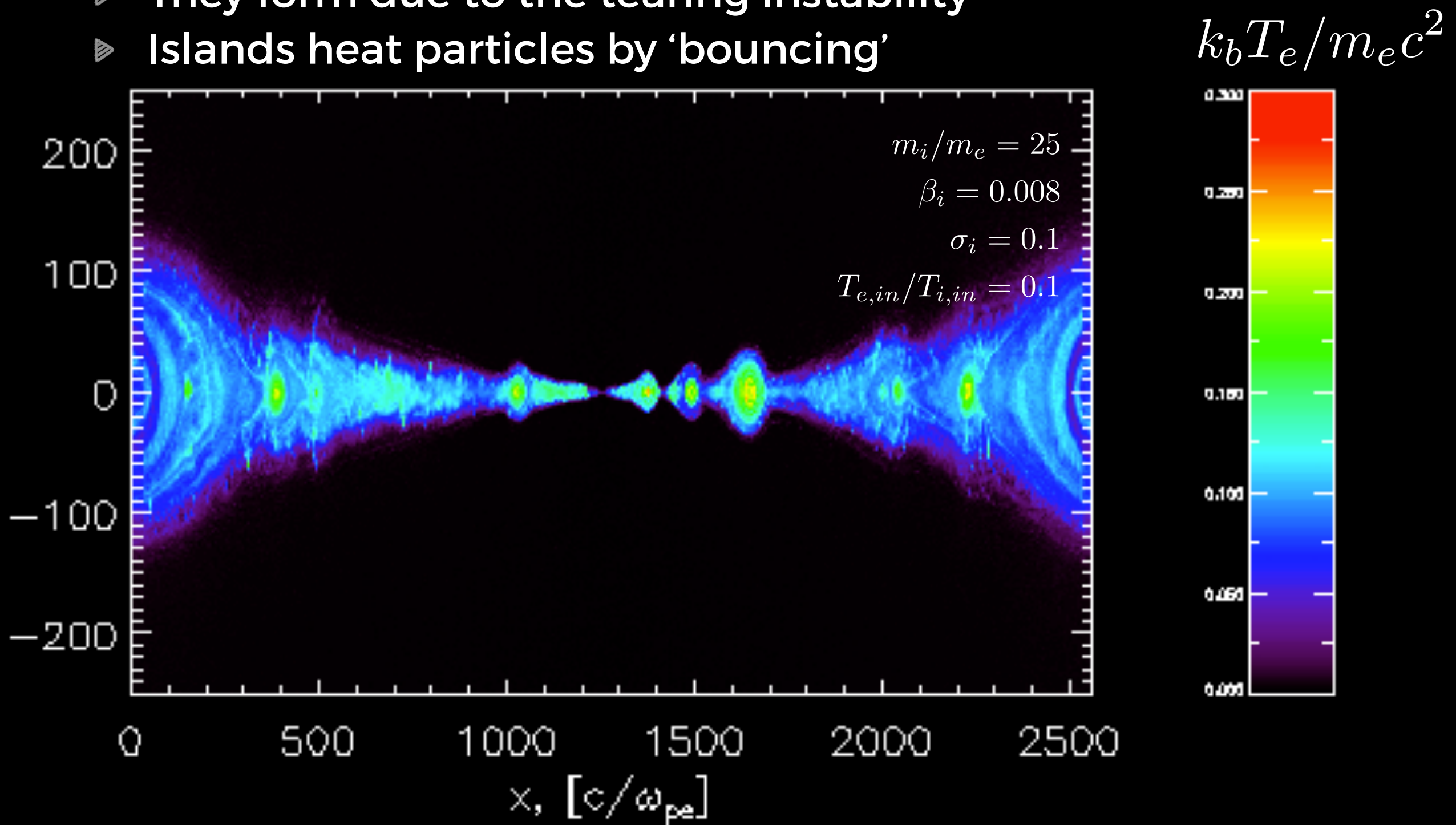


Tag particles on right

Region selected is insensitive to the particular threshold value

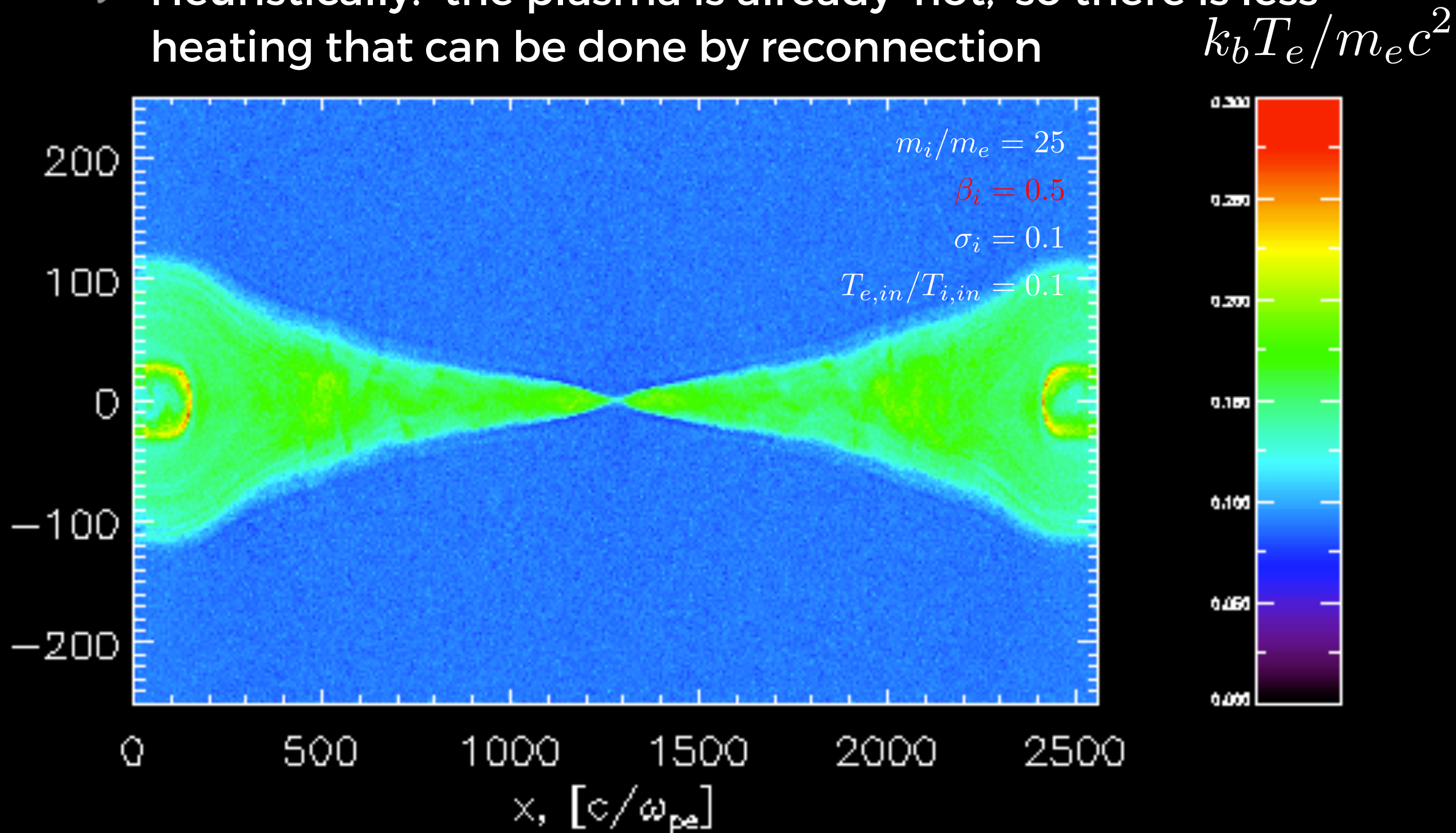
# This is a low-beta plasma...

- ▶ The circular substructures are ‘magnetic islands’
- ▶ They form due to the tearing instability
- ▶ Islands heat particles by ‘bouncing’



# ...and this is a high(er)-beta plasma

- ▶ Islands are absent; thermal pressure suppresses tearing mode
- ▶ Heuristically: the plasma is already ‘hot,’ so there is less heating that can be done by reconnection



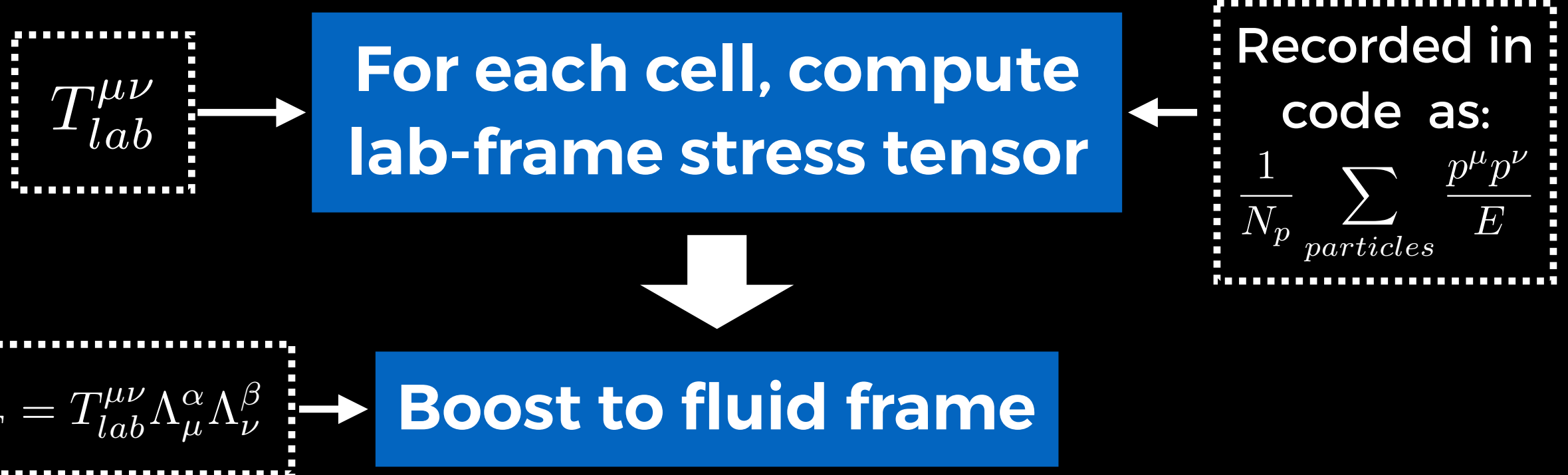
# We carefully extract the temperature increase

$$T_{lab}^{\mu\nu}$$

For each cell, compute  
lab-frame stress tensor

Recorded in  
code as:  
$$\frac{1}{N_p} \sum_{particles} \frac{p^\mu p^\nu}{E}$$

# We carefully extract the temperature increase



# We carefully extract the temperature increase

$$T_{lab}^{\mu\nu}$$

For each cell, compute  
lab-frame stress tensor

Recorded in  
code as:  
$$\frac{1}{N_p} \sum_{particles} \frac{p^\mu p^\nu}{E}$$

$$T_{CMRF}^{\alpha\beta} = T_{lab}^{\mu\nu} \Lambda_\mu^\alpha \Lambda_\nu^\beta$$

Boost to fluid frame

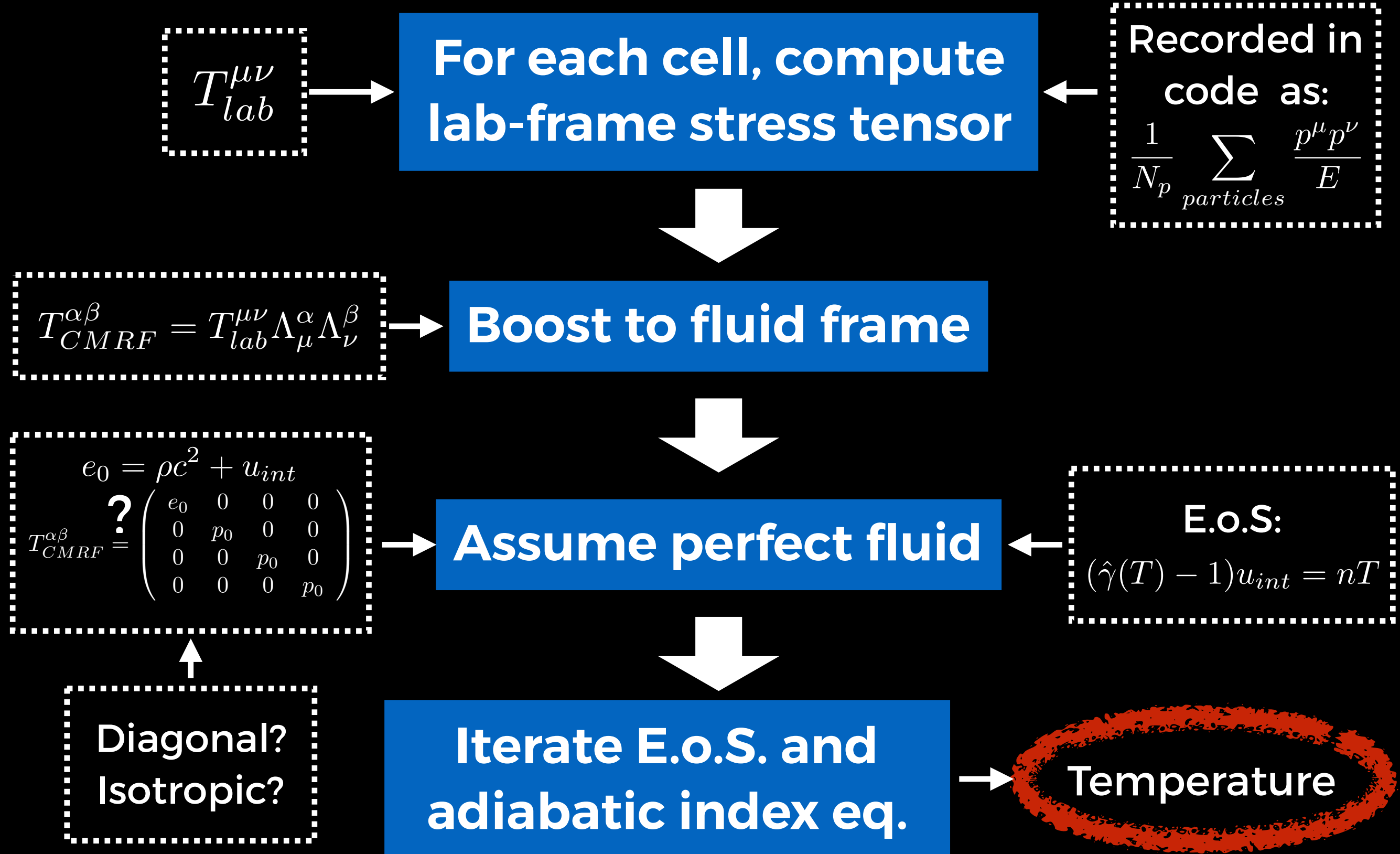
$$e_0 = \rho c^2 + u_{int}$$
$$T_{CMRF}^{\alpha\beta} = ? \begin{pmatrix} e_0 & 0 & 0 & 0 \\ 0 & p_0 & 0 & 0 \\ 0 & 0 & p_0 & 0 \\ 0 & 0 & 0 & p_0 \end{pmatrix}$$

Assume perfect fluid

E.o.S:  
 $(\hat{\gamma}(T) - 1)u_{int} = nT$

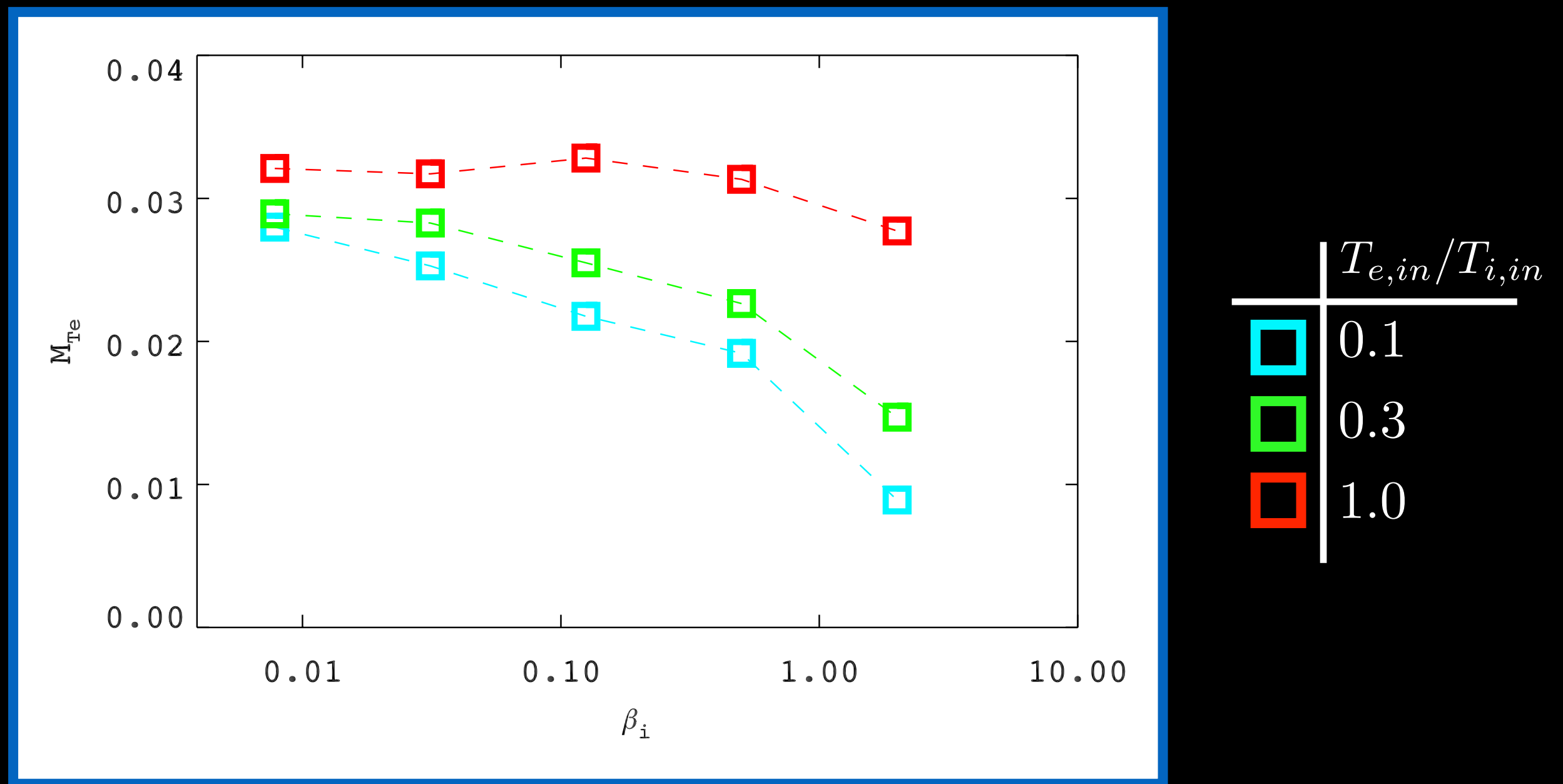
Diagonal?  
Isotropic?

# We carefully extract the temperature increase



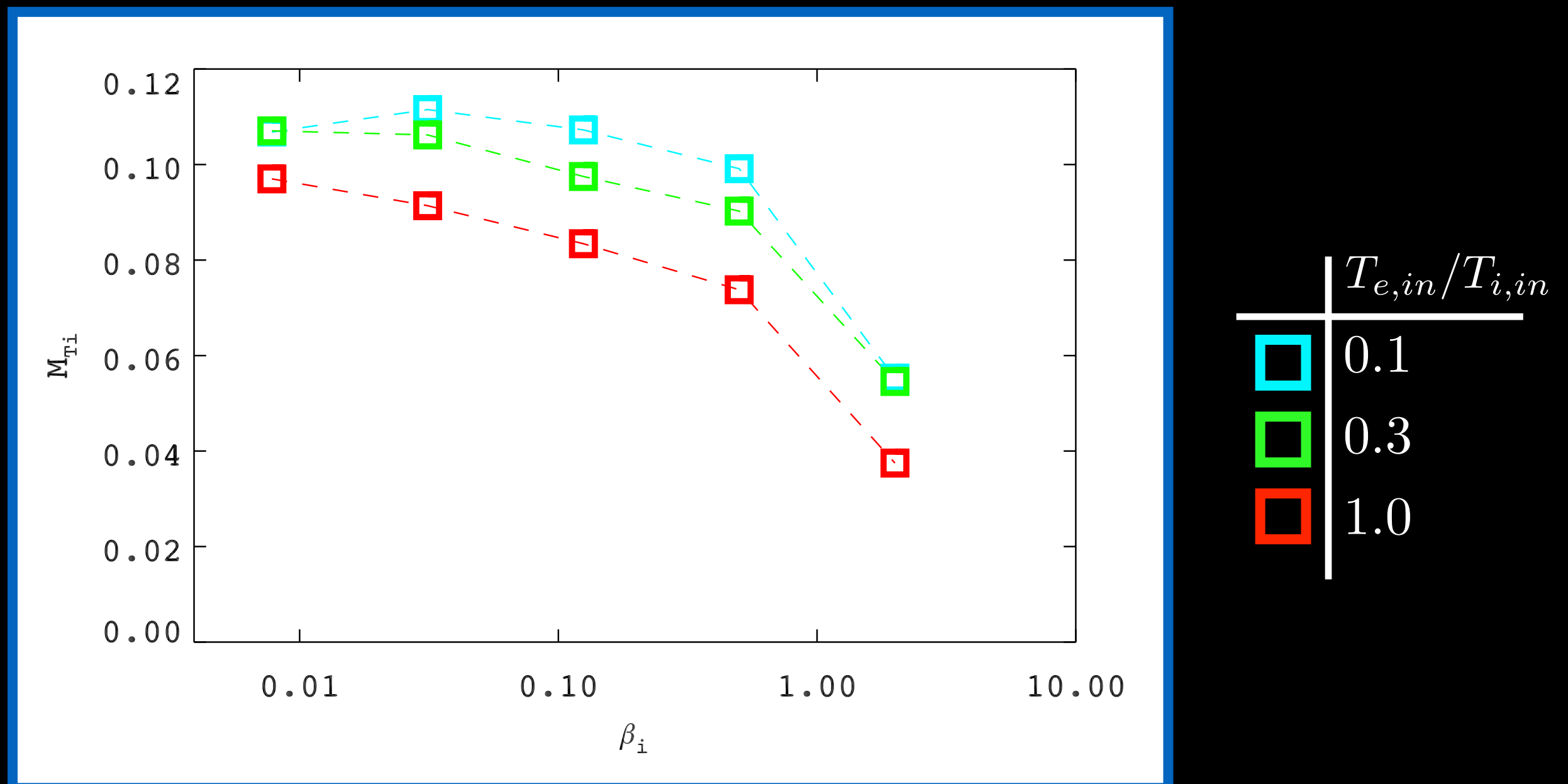
# Electron gross heating

- ▶ For low-beta, the fraction of magnetic energy that ends up as electron heating is around 3%
- ▶ Dependence on initial temperature ratio



# Ion gross heating

- ▶ Free magnetic energy that ends up as ion heating: ~10-12%
- ▶ This gives us a rough value for electron:ion heating as 1/3 in the low-beta cases



# Compressive vs. non-compressive heating

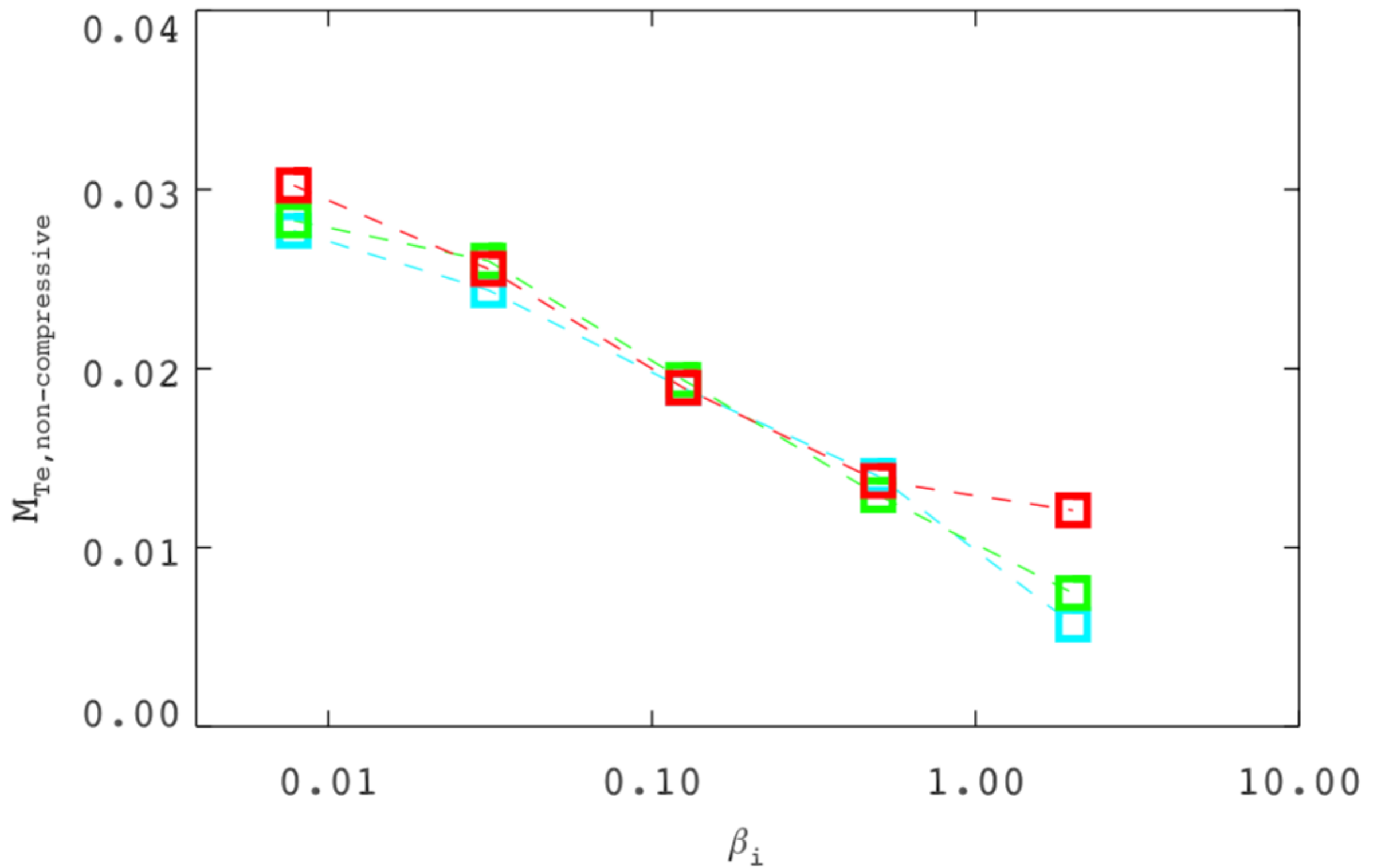
- ▶ We use the following equation of state to account for the fact that electrons' adiabatic index can vary from beginning to end of reconnection:

## Equation of state for variable adiabatic index

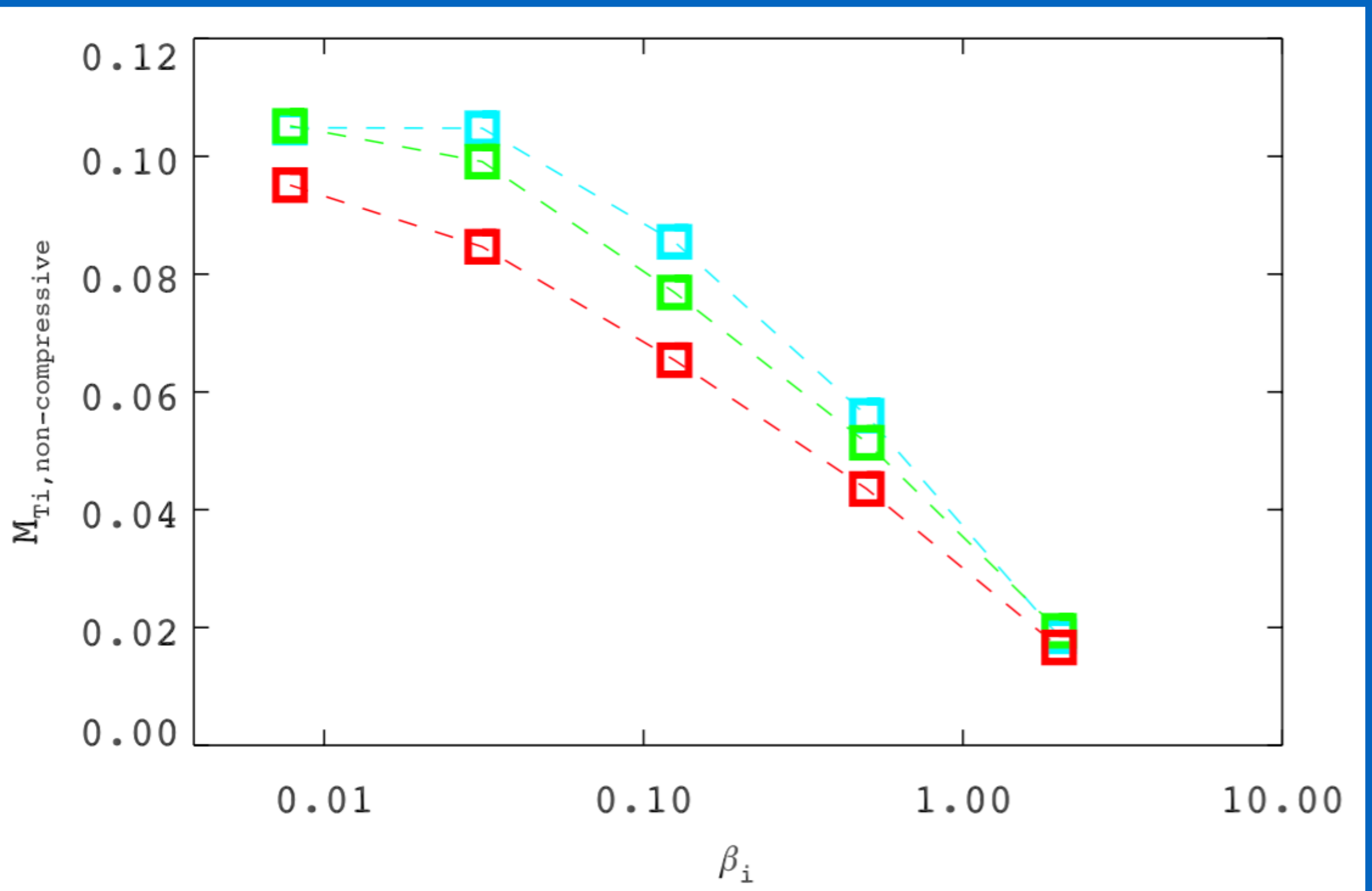
$$const = \frac{p}{\rho^{5/3}} \left( \frac{3}{2} \Theta + \sqrt{\frac{9}{4} \Theta^2 + 1} \right), \Theta = \frac{kT}{mc^2}$$

- ▶ This allows us to remove the compressive component of the heating, which is not a result of heating due to the reconnection electric field

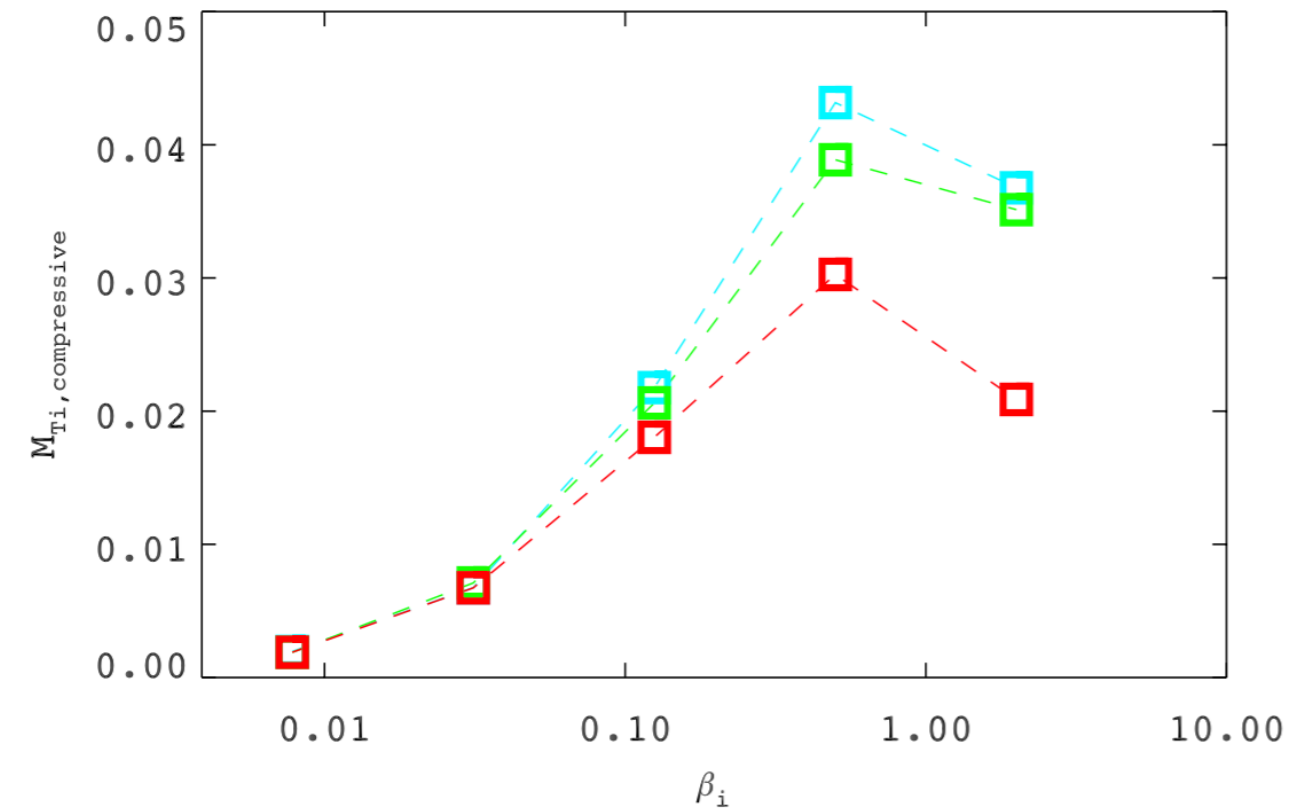
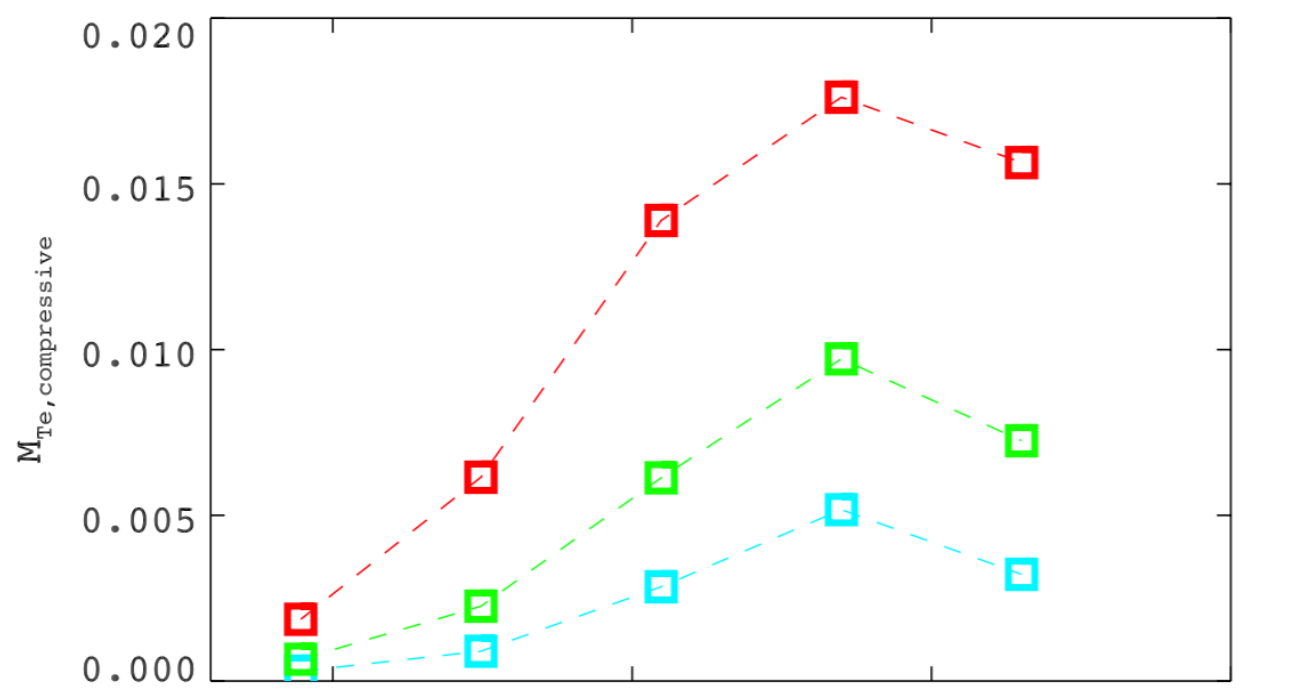
# Electrons: heating analysis



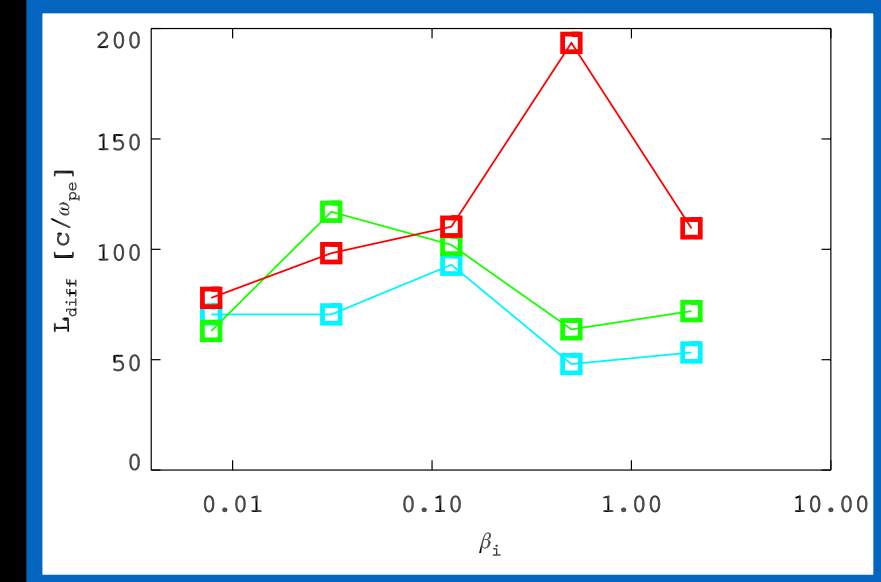
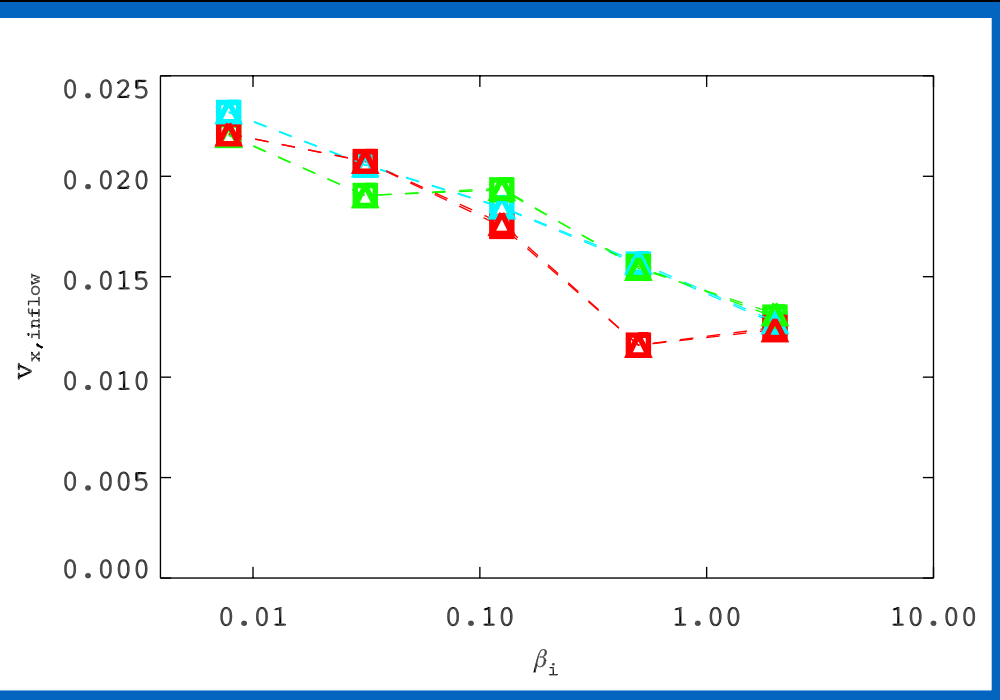
# Ions: heating analysis



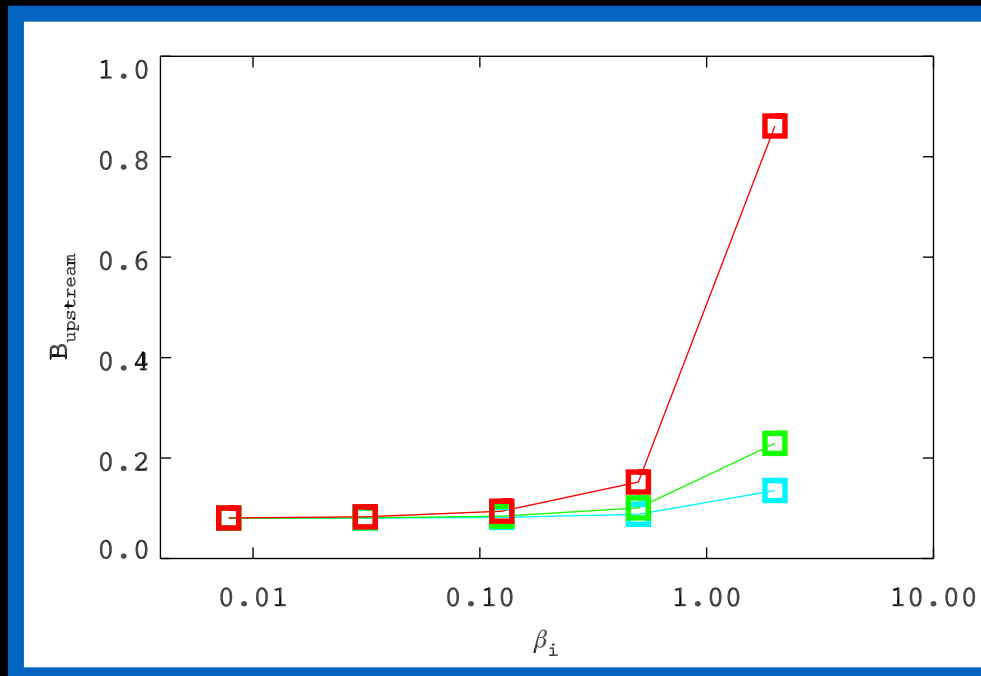
# Compressive heating



# A simple model for the electron heating

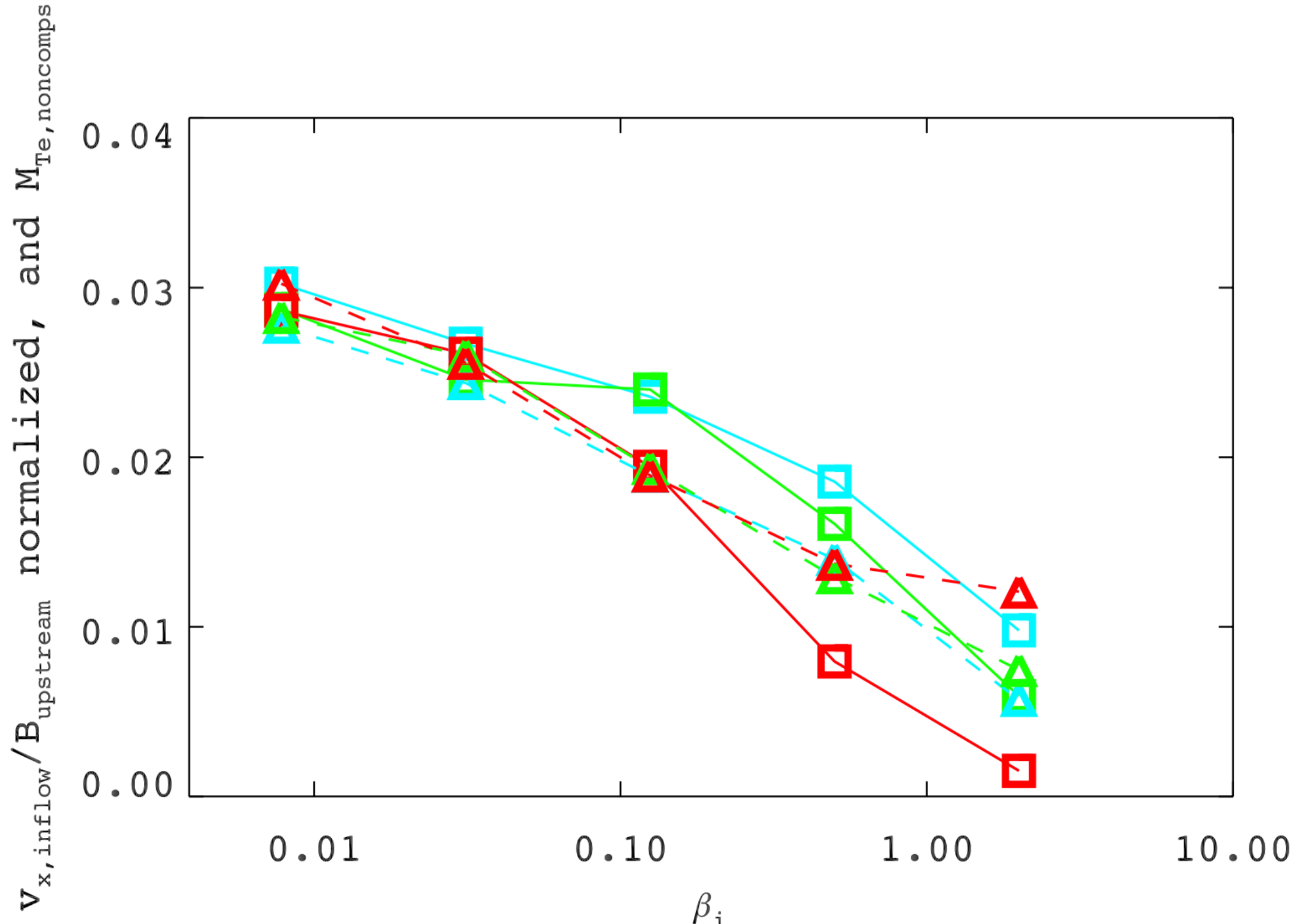


$$M_{Te,ideal} \sim \frac{eE_{rec}Ln}{B^2/8\pi} \sim \boxed{\frac{e \left( \frac{v_{in}}{c} \right) Ln}{B}}$$



- ▶ The expression is roughly the work done by reconnection E field compare to inflow magnetic energy
- ▶ Treat B, L, and  $v_{in}$  as functions of beta,  $T_e/T_i$  - don't just assume constant

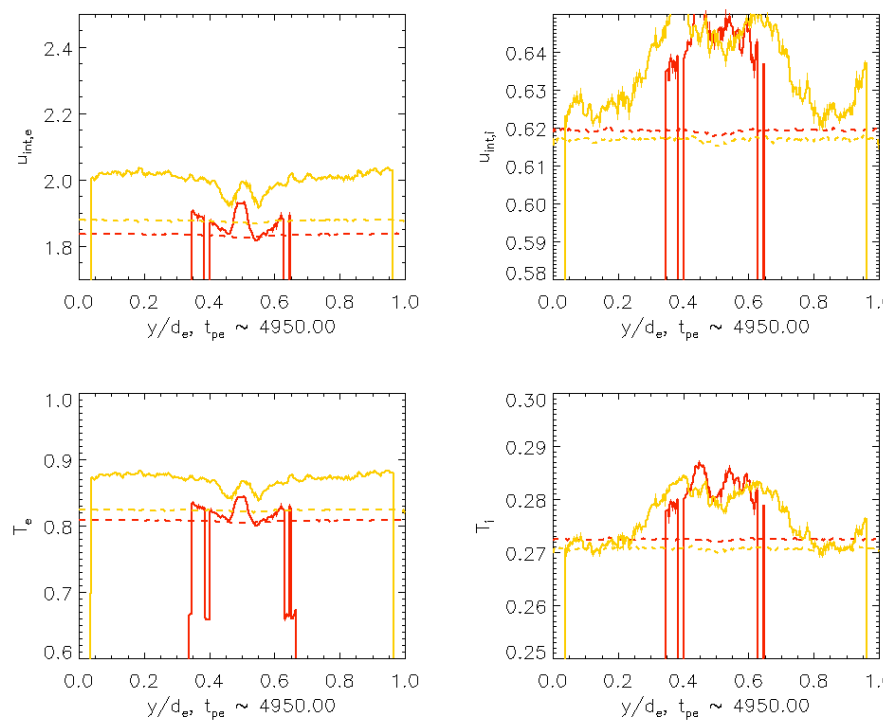
# Diffusion region heating vs. model



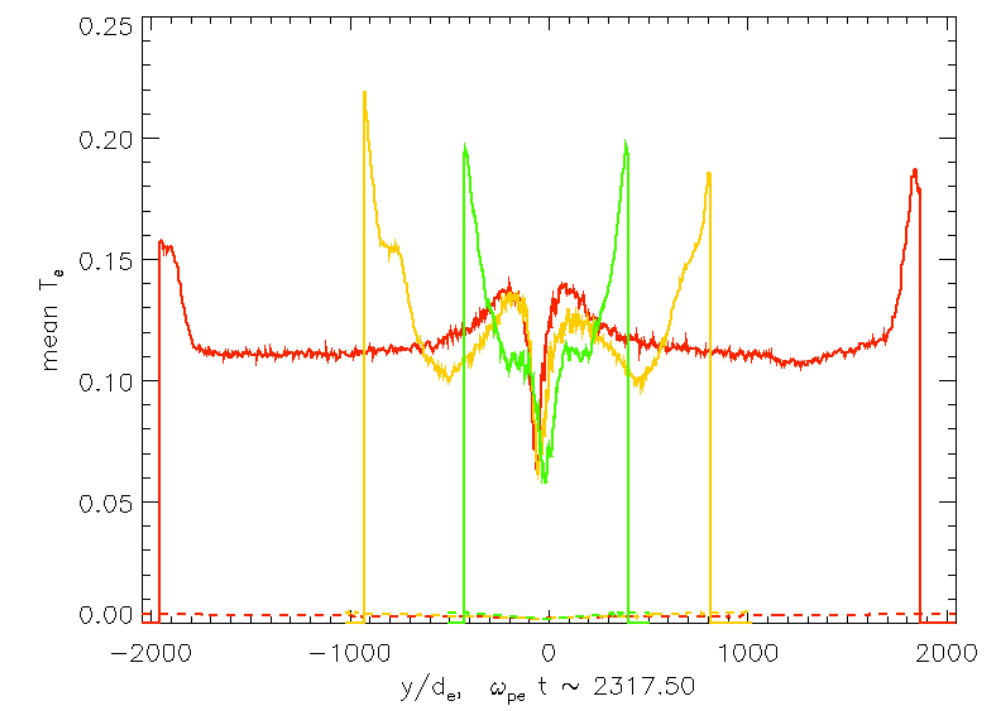
# Heating should not depend on nonphysical parameters

- ▶ Check for convergence by varying computational parameters
- ▶ To trust the numerical results, need to make sure numerical heating is relatively small
- ▶ Particles per cell, domain size, boundary conditions, etc.

**ppc = 64 (yellow), ppc = 256 (red)**



**$m_y = 4096$  (green),  $8192$  (yellow),  $16384$**

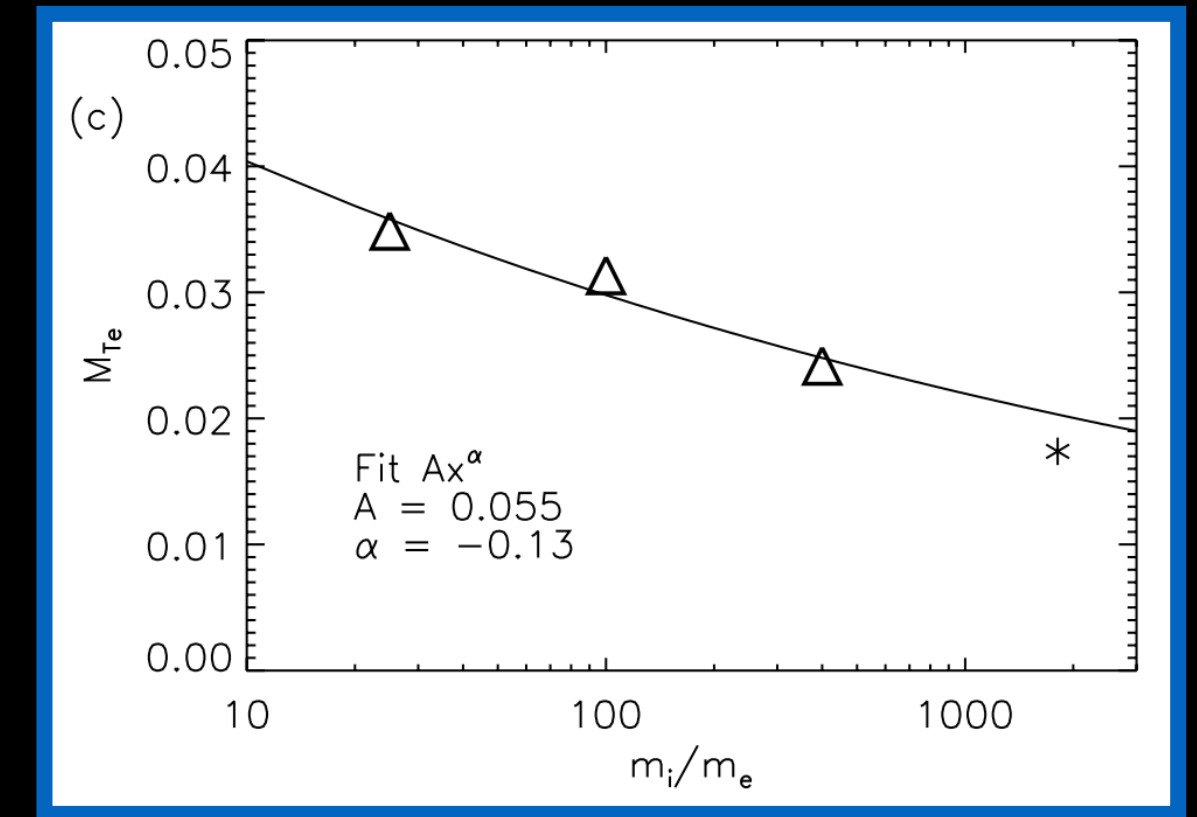


# Electron heating will decrease with higher $m_i/m_e$

- ▶ In our simulations, we use an artificial mass ratio of  $m_i/m_e = 25$ 
  - ▶ Why? This makes the problem computationally tractable
- ▶ We can expect our measured heating will decrease with higher mass ratio;

$$M_{Te} \sim (m_i/m_e)^{-0.13}$$

(Drake et al., 2014)



- ▶ Note: this scaling is consistent with the analytical model of Egedal et al.

# Connection to black-hole physics

- ▶ Two main aspects to our investigation
  - ▶ Plasma physics
    - ▶ Explore a relatively unstudied region of plasma parameter space
  - ▶ Astrophysics
    - ▶ Provide (eventually) a lookup table for global simulations of black-hole accretion flows
    - ▶ Even if it turns out that the dependence on input values is weak, at least this will be known from a first-principles investigation

# Summary and future directions

## Summary:

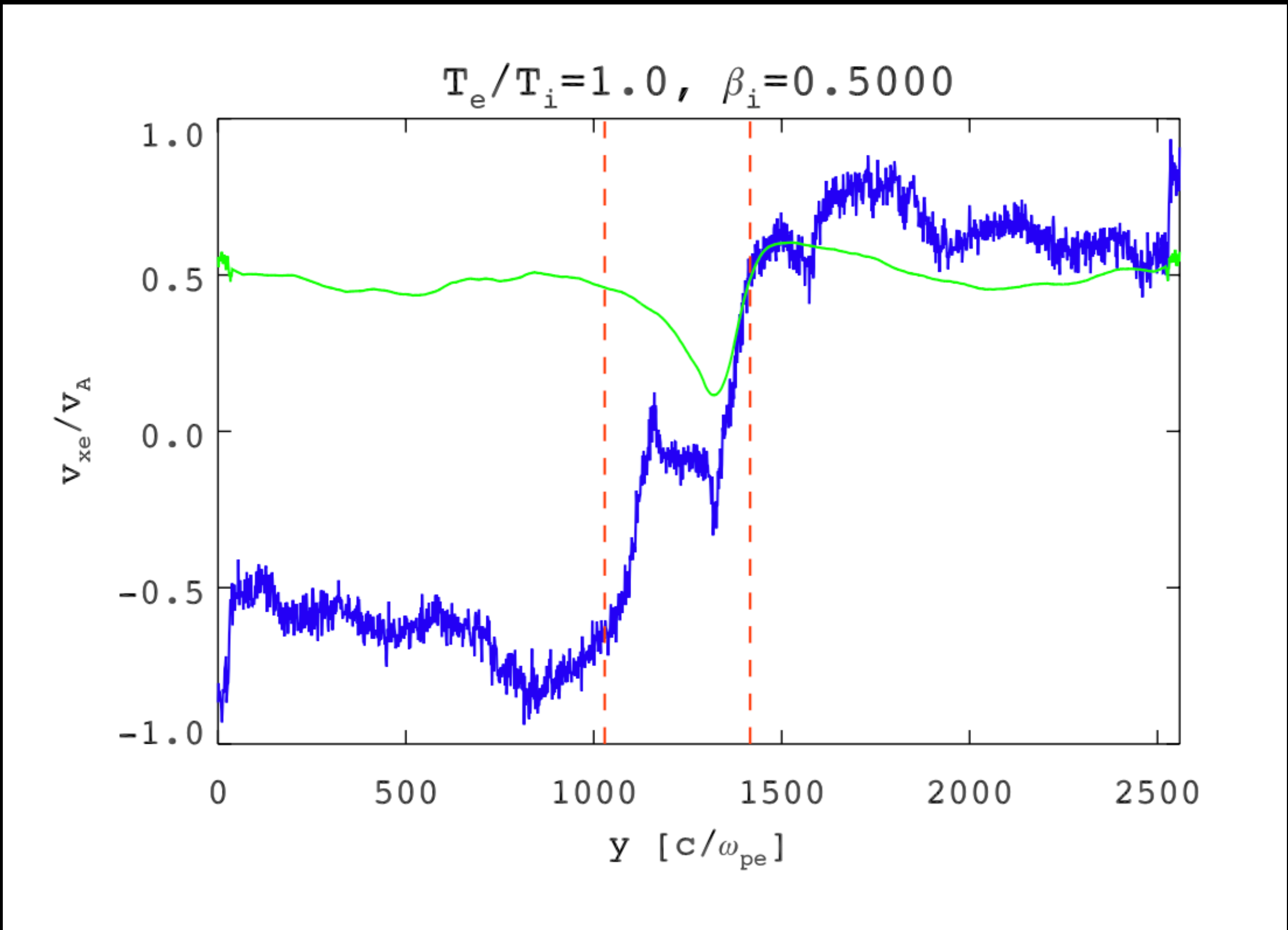
- ▶ Reconnection provides less net heating for high-beta compared to low-beta;  $T_{e,\text{out}} / T_{e,\text{in}}$  approaches 1 for high beta
- ▶ Low-beta: ~3% of the magnetic energy ends up as electron heating, and ~10-12% ends up as ion heating

## For the future:

- ▶ Explore guide field reconnection
- ▶ Push to higher beta
- ▶ Vary the mass ratio
- ▶ Run with wider range of sigma
- ▶ Use particle orbits to study heating mechanism
  - ▶ Is this the same as in the non-relativistic case?
- ▶ 3D simulations

Thank you for your attention

# Strange-looking point from plot of L(beta)



# E.o.S. derivation

What is our equation of state if the adiabatic index is not constant?

$$dS = \frac{dQ}{\Theta}, dQ = dH - Vdp, \Theta = \frac{p}{\rho}$$

$$\Rightarrow dS = \frac{dH}{\Theta} - V \frac{dp}{\Theta} = \frac{dH}{\Theta} - \frac{N}{p} dp$$

$$dS = \frac{dh}{\Theta} - d \log p$$

Now integrate, using equation for  $h(\Theta)$ :

$$h = \frac{5}{2}\Theta + \sqrt{\frac{9}{4}\Theta^2 + 1}$$

$$\Rightarrow \int dS = \int \frac{1}{\Theta} \left( \frac{5}{2} + \left( \frac{9}{4}\Theta^2 + 1 \right)^{-1/2} \frac{9}{4}\Theta \right) d\Theta - \log p$$

$$S = \frac{5}{2} \log \Theta + \frac{3}{2} \sinh^{-1} \left( \frac{3}{2}\Theta \right) - \log p$$

$$= \frac{5}{2} \log \Theta + \frac{3}{2} \log \left( \frac{3}{2}\Theta + \sqrt{\left( \frac{3}{2}\Theta \right)^2 + 1} \right) - \log p$$

$$= \frac{3}{2} (\log \Theta + \log (h - \Theta)) + \log \left( \frac{\Theta}{p} \right)$$

$$= \frac{3}{2} \log \left( \frac{\Theta^{5/3}}{p^{2/3}} (h - \Theta) \right)$$

$$= \frac{3}{2} \log \left( \frac{p}{\rho^{5/3}} (h - \Theta) \right)$$

$$const = \frac{p}{\rho^{5/3}} \left( \frac{3}{2}\Theta + \sqrt{\frac{9}{4}\Theta^2 + 1} \right)$$

This provides the correct limiting values. For  $\Theta \rightarrow 0$ ,

$$const = \frac{p}{\rho^{5/3}}$$

and for  $\Theta \gg 1 \Leftrightarrow p \gg \rho$ ,

$$const \simeq \frac{p}{\rho^{5/3}} 3\Theta$$

$$\Rightarrow const' = \frac{p^2}{\rho^{8/3}}$$

$$\Rightarrow const'' = \frac{p}{\rho^{4/3}}$$

The adiabatic index is not the same in the upstream as compared to outflow region. To make a meaningful comparison of the compressive heating, we should compute  $const$  upstream, then use the variable equation of state (boxed above) to compute the predicted value  $const$  for given  $\Theta, p, \rho$  in the outflow. Discrepancy between the predicted and actual values should then be accounted for by ‘actual’ heating.

The equation we used for specific enthalpy comes from Taub inequality, taking the equals sign:

$$(h - \Theta)(h - 4\Theta) \geq 0$$

$$\Rightarrow h^2 - h5\Theta + 4\Theta^2 - 1 \geq 0$$

$$\Rightarrow h = \frac{5}{2} + \sqrt{\frac{9}{4}\Theta^2 + 1}$$

# Sgr A\* radiation spectrum

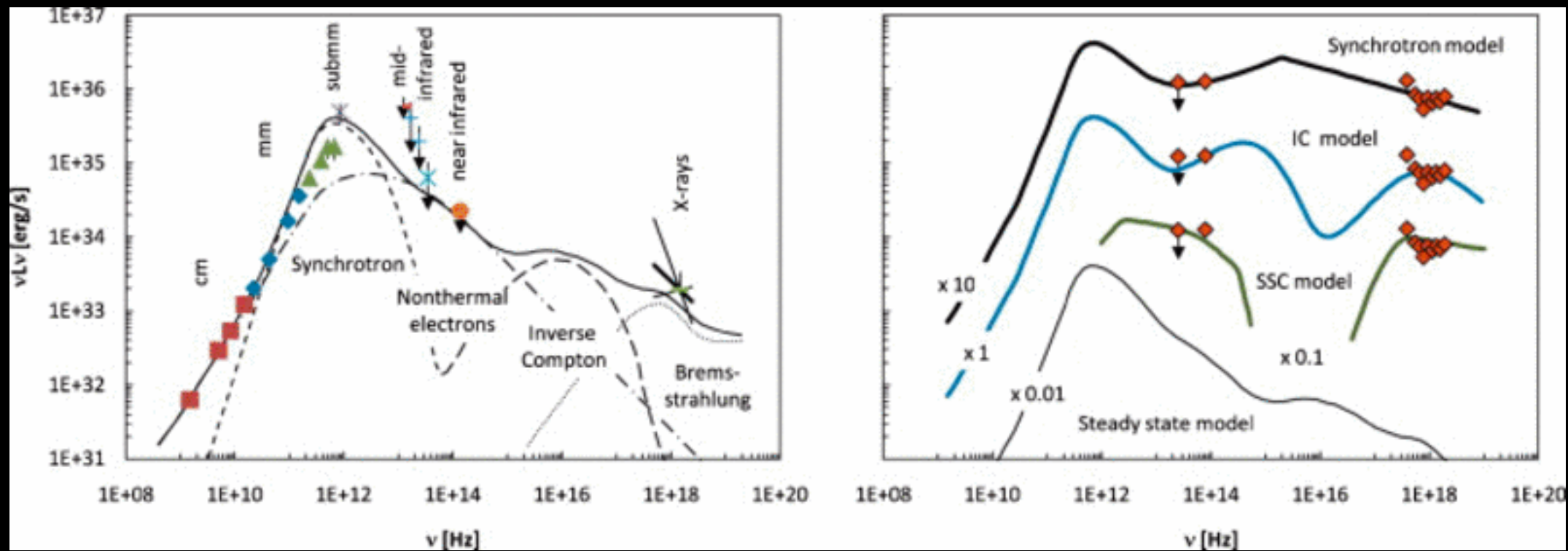


Figure 30(Color) Spectral energy distribution of Sgr A\*. All numbers are given for a distance of 8.3kpc of the Galactic Center and are dereddened for interstellar absorption (infrared and x rays) and scattering (x rays). Left: steady state. The Sgr A\* radio spectrum follows roughly a power law  $\nu L_\nu \sim \nu^{4/3}$ . The observed peak flux at submillimeter wavelengths is about  $5 \times 10^{35} \text{ erg/s}$ . The spectrum then steeply drops toward infrared wavelengths down to less than the detection limit of about  $2 \times 10^{34} \text{ erg/s}$  at  $2\mu\text{m}$ . The only other unambiguous detection of Sgr A\* in its steady state is at x rays with energies from 2–10keV with a flux of about  $2 \times 10^{33} \text{ erg/s}$ . The figure shows a compilation of data (with increasing frequency) from ■ (560), ◆ (150), ▲ (565), × (487), - (105), + (186), × (475), ● (243), and – (34). Overplotted is a model of the quiescent emission [adapted from 541]: the radio spectrum is well described by synchrotron emission of thermal electrons (short-dashed line). The flattening of the radio spectrum at low frequency is modeled by the additional emission from a nonthermal power-law distribution of electrons, which carry about 1.5% of the total thermal energy (dash-dotted line). The quiescent x-ray emission arises from thermal bremsstrahlung from the outer parts of the accretion flow (dotted line). The secondary maximum (long-dashed line) at frequencies of about 10<sup>16</sup>Hz is the result of the inverse Compton upscattering of the synchrotron spectrum by the thermal electrons. Right: SED during a simultaneous x ray and infrared flare: while the total

# 1. Solve for the fields

- In electromagnetic PIC codes, only two equations need to be solved.

- The other two are satisfied as initial conditions, and they continue to be satisfied for appropriate choices of the numerical scheme.

$$\begin{aligned}\partial_t \mathbf{B} &= -\nabla \times \mathbf{E}, \\ \partial_t \mathbf{E} &= \nabla \times \mathbf{B} - \mathbf{J}.\end{aligned}$$

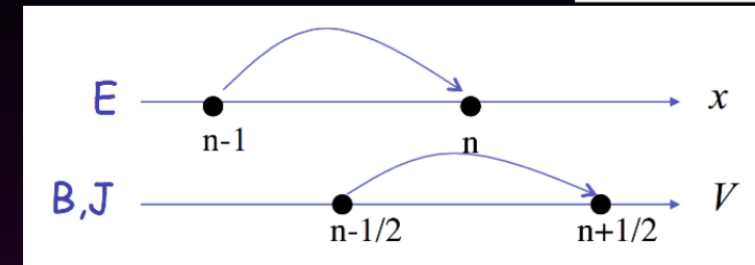
$$\begin{aligned}\nabla \cdot \mathbf{E} &= \rho, \\ \nabla \cdot \mathbf{B} &= 0.\end{aligned}$$

STAGGERING in time (leapfrog):

- second-order accurate in time

$$E^{n+1/2} = E^{n-1/2} + \Delta t [c(\nabla \times B^n) - 4\pi J^n]$$

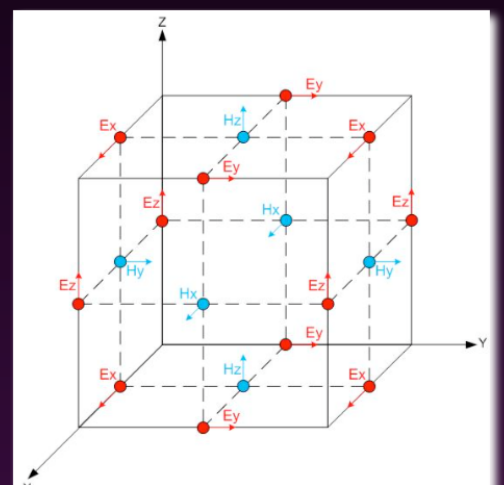
$$B^{n+1} = B^n - c\Delta t \nabla \times E^{n+1/2}.$$



STAGGERING in space (Yee's mesh):

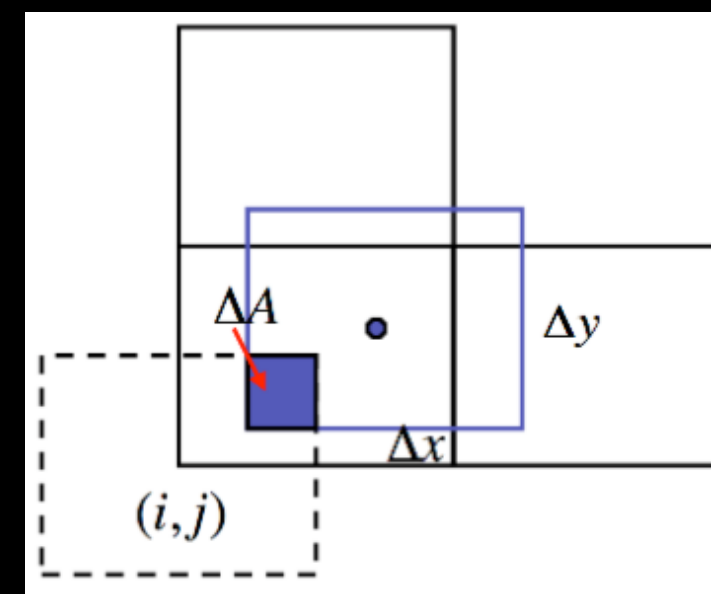
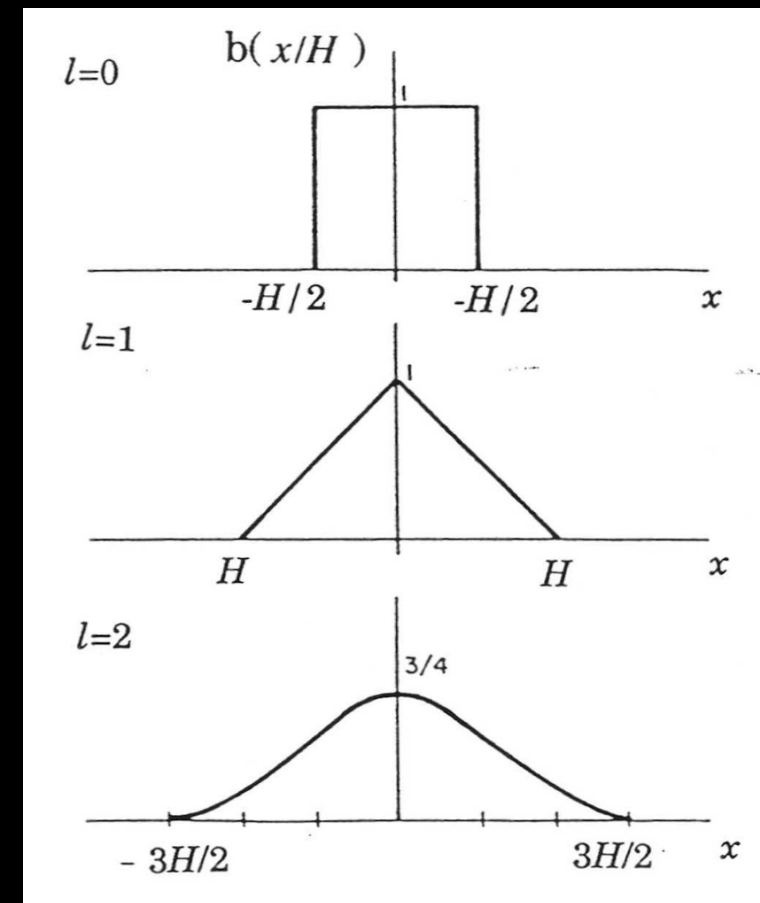
- electric fields on cell edges, magnetic fields on cell faces
- second-order accurate in space
- maintains divergence-free B

$$\begin{aligned}\partial_t \mathbf{B} &= -\nabla \times \mathbf{E}, \\ \partial_t \mathbf{E} &= \nabla \times \mathbf{B} - \mathbf{J}\end{aligned}$$



## 2. Interpolate fields to particle positions

- The fields obtained from Maxwell's equations are determined only at the grid points, they need to be interpolated to the particle positions.
- The interpolation is done by assuming a particle shape function.
- The shape function needs to be:
  1. isotropic
  2. zero outside some range
  3. higher order B-splines are computationally more expensive, but more accurate and less “collisional”



$$E(\vec{x}_k) = \sum_{i,j} E_{ij} S(\vec{x}_k - \vec{X}_{ij})$$

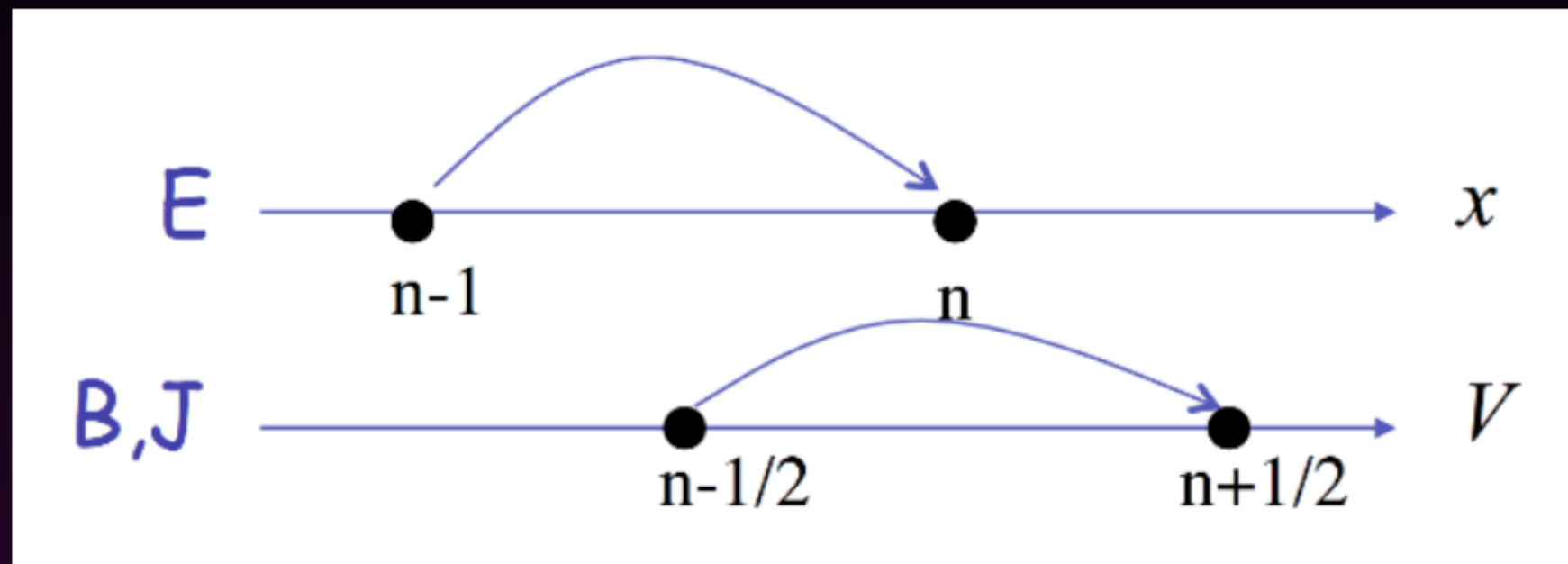
$$S(\vec{x}_k - \vec{X}_{ij}) = \frac{\Delta A}{\Delta x \Delta y}$$

$$\sum_{i,j} S(\vec{x}_k - \vec{X}_{ij}) = 1$$

### 3. Push the particles

If the number of ppc is  $\gg 1$ , most of the computing time is spent in pushing the particles.

The BORIS pusher (leapfrog method)



advance the position

$$x^{n+1} = x^n + \frac{p^{n+1/2}}{\gamma^{n+1/2}} \Delta t$$

advance the momentum

$$\frac{p^{n+1/2} - p^{n-1/2}}{\Delta t} = \frac{q}{m} (E^n + \frac{1}{c} \frac{p^{n+1/2} + p^{n-1/2}}{2\gamma^n} \times B^n)$$
$$(B^n = \frac{B^{n+1/2} + B^{n-1/2}}{2})$$

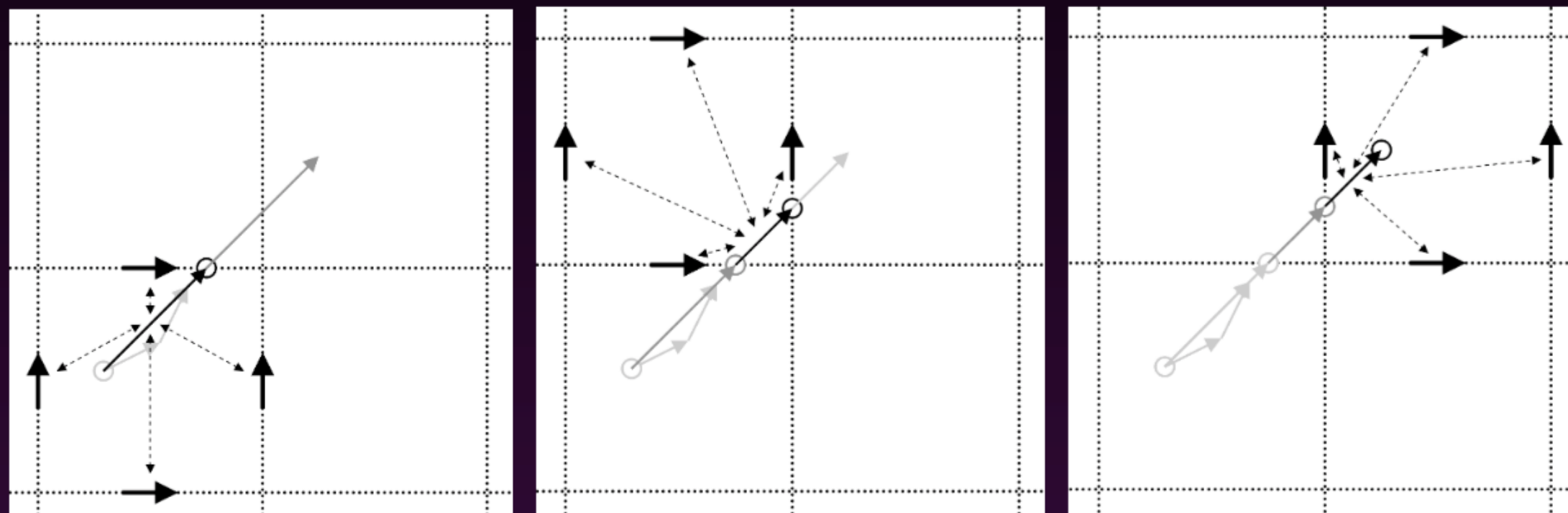
## 4. Deposit current on the grid

- Charge conservation is required to satisfy Poisson's equation.

$$\partial_t B = -\nabla \times E \Rightarrow \partial_t \nabla \cdot B = 0$$

$$\partial_t E = \nabla \times B - J \Rightarrow \partial_t \nabla \cdot E = -\nabla \cdot J \xrightarrow{?} \partial_t \rho$$

- The current deposition scheme needs to be charge-conserving.



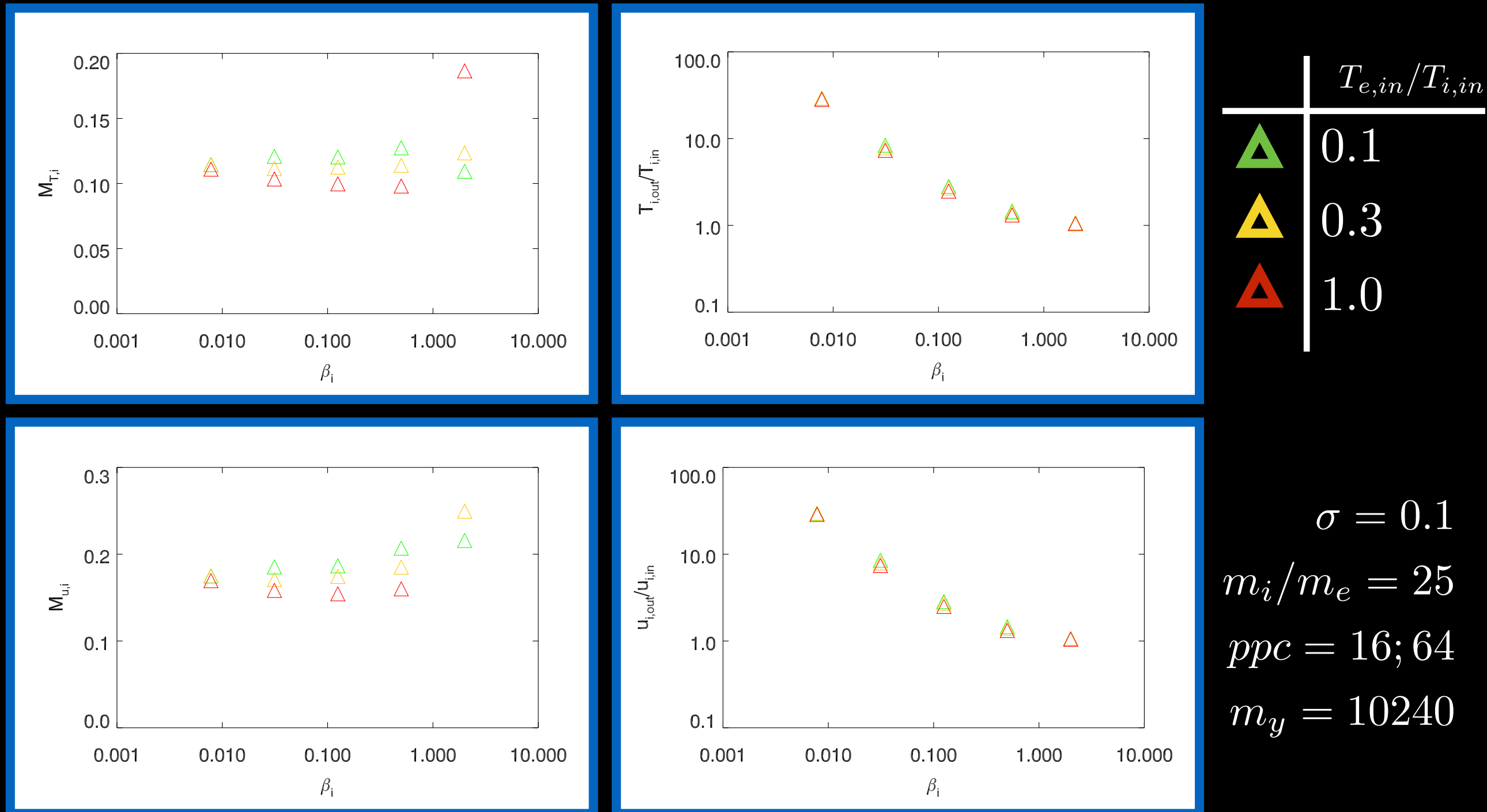
- Or, a divergence-cleaning solver should be employed.

# Numerical stability

- The particle granularity gives short-scale fluctuations of the electromagnetic fields, whose mean amplitude scales (Poisson-like) as  $\sqrt{n}$ , where  $n$  is the particle density.
- The fractional contribution of the fluctuations (over the slowly varying fields) scales as  $1/\sqrt{n}$ .
- This is problematic because the number of super-particles in particle-in-cell codes is  $\ll$  number of real particles.
- We need to control the level of the fluctuations such that they give negligible effects over the timespan of the simulations.

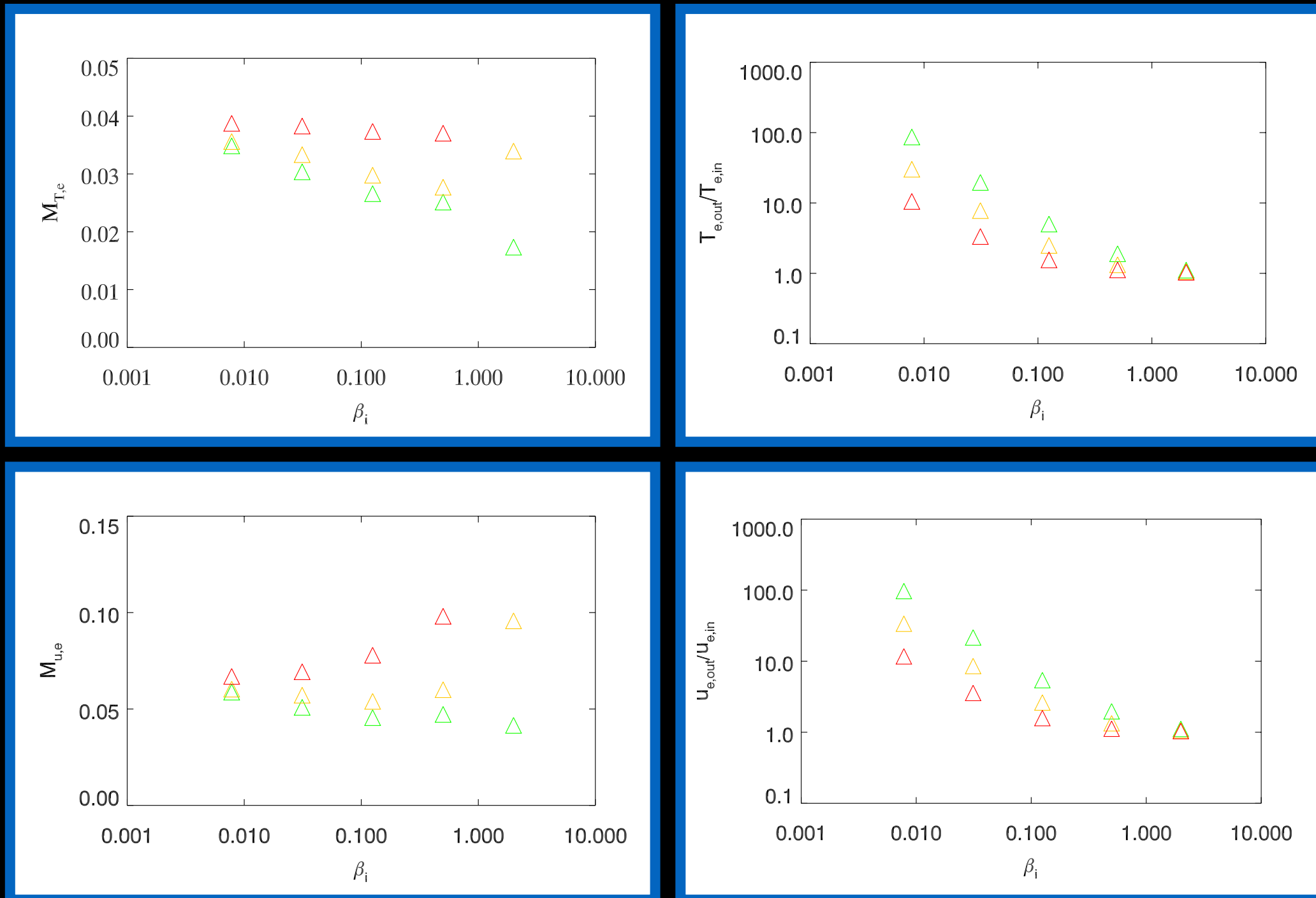
# Ion heating I

For completeness, here are the corresponding ion plots:



# Electron heating I

The particle heating can be characterized in different ways:



$\sigma = 0.1$   
 $m_i/m_e = 25$   
 $ppc = 16; 64$   
 $m_y = 10240$

# Electron vs. Ion heating

